Supporting Information for: Ionic Conductivity, Structural Deformation and Programmable Anisotropy of DNA Origami in Electric Field

Chen-Yu Li,[†] Elisa A. Hemmig,[‡] Jinglin Kong,[‡] Jejoong Yoo,[¶] Silvia Hernández-Ainsa,[‡] Ulrich F. Keyser,[*,‡] and Aleksei Aksimentiev[*,§]

Center for Biophysics and Computational Biology, University of Illinois at Urbana–Champaign, Cavendish Laboratory, University of Cambridge, UK, Center for the Physics of Living Cells, University of Illinois at Urbana–Champaign, and Department of Physics, University of Illinois at Urbana–Champaign, USA

E-mail: ufk20@cam.ac.uk; aksiment@illinois.edu

KEYWORDS: Nanopore, DNA nanotechnology, ionic current, molecular dynamics, FRET, DNA sequencing

[*]To whom correspondence should be addressed
[†]Center for Biophysics and Computational Biology, University of Illinois at Urbana–Champaign
[‡]Cavendish Laboratory, University of Cambridge, UK
[¶]Center for the Physics of Living Cells, University of Illinois at Urbana–Champaign
[§]Department of Physics, University of Illinois at Urbana–Champaign, USA

Supporting Methods

Ionic current calculations. Prior to calculations of the ionic current, frames of the MD trajectory were aligned to have the center of mass of the DNA origami stationary. Doing so eliminated the noise associated with the system's drift. The instantaneous current was computed as

$$I(t+\frac{\Delta t}{2}) = \frac{1}{\Delta t L_{\mathrm{z}}} \sum_{i}^{N} q_i \Delta z_i \tag{1}$$

where the sum over i indicates a sum over all ions, Δt is the time interval between the two consecutive frames of the trajectory, L_{z} is the length of the system along the z axis, q_i is the charge of ion i and $\Delta z_i = z_i(t+\Delta t) - z_i(t)$ is the displacement of ion i along the z direction between the two frames.[1] To properly account for the wrapping of the MD trajectory according to the periodic boundary conditions,

$$\Delta z_i = \begin{cases} z_i(t+\Delta t) - z_i(t) - L_{\mathrm{z}}, & z_i(t+\Delta t) - z_i(t) > L_{\mathrm{z}}/2 \\ z_i(t+\Delta t) - z_i(t) + L_{\mathrm{z}}, & z_i(t+\Delta t) - z_i(t) < -L_{\mathrm{z}}/2. \end{cases} \tag{2}$$

The average current of a trajectory was computed by summing up all instantaneous currents and dividing by the number of coordinate frames of the trajectory. Typically, the frames were collected every 2.4 ps. To estimate the error, the ionic current trace was first block averaged, using, as the block size, the autocorrelation time of the current. For the set of instantaneous current values $\{I_1, I_2, \cdots, I_n\}$, the autocorrelation function

$$R(k) = \frac{1}{(n-k)\sigma^2} \sum_{i=1}^{n-k} (I_i - \mu)(I_{i+k} - \mu), \tag{3}$$

for any positive integer $k < n$. In the above expression, n is the total number of instantaneous current values in the dataset, μ and σ^2 are the mean and the variance of the dataset, respectively. We define the autocorrelation time as the smallest k which satisfies $R(k) = 0$. The reported standard errors of the mean were calculated from the block-averaged current traces.

Calculations of the local flux. The local three-dimensional (3D) flux of ions and water was computed by extending the method described in the previous section to 3D. The change in the coordinates of particle i between consecutive frames is

$$\Delta\mathbf{r}_i(t+\Delta t/2) = (\Delta x_i(t+\Delta t/2), \Delta y_i(t+\Delta t/2), \Delta z_i(t+\Delta t/2)), \tag{4}$$

where $\Delta x_i(t+\Delta t/2)$ and $\Delta y_i(t+\Delta t/2)$ are computed similarly to $\Delta z_i(t+\Delta t/2)$, Eq. 2. To compute local fluxes, we used a regular orthogonal $N_x \times N_y \times N_z$ grid dividing the simulation box into $N_x \times N_y \times N_z$ rectangular blocks of identical dimensions $l_x = L_x/N_x$, $l_y = L_y/N_y$ and $l_z = L_z/N_z$. A set of indices (l,m,n) indicates the position of each block in x, y, and z directions. To compute the contribution of the displacement vector of particle i, $\Delta\mathbf{r}_i(t+\Delta t/2)$, to the local flux through each block, we assumed that the particle migrates from $\mathbf{r}_i(t)$ to $\mathbf{r}_i(t+\Delta t)$ along a straight line. Then, we determined the fraction of the displacement vector in each of the $N_xN_yN_z$ blocks, $f_{i,(l,m,n)}(t+\Delta t/2)$ such that $\sum_l \sum_m \sum_n f_{i,(l,m,n)}(t+\Delta t/2) = 1$. Finally, we defined the components of the instantaneous local flux per unit area of a chosen species in block (l,m,n) as

$$\begin{aligned}
J_{x,(l,m,n)}(t+\Delta t/2) &= \tfrac{1}{\Delta t l_x l_y l_z} \textstyle\sum_i^M \Delta x_i(t+\Delta t/2) f_{i,(l,m,n)}(t+\Delta t/2) \\
J_{y(l,m,n)}(t+\Delta t/2) &= \tfrac{1}{\Delta t l_x l_y l_z} \textstyle\sum_i^M \Delta y_i(t+\Delta t/2) f_{i,(l,m,n)}(t+\Delta t/2) \\
J_{z,(l,m,n)}(t+\Delta t/2) &= \tfrac{1}{\Delta t l_x l_y l_z} \textstyle\sum_i^M \Delta z_i(t+\Delta t/2) f_{i,(l,m,n)}(t+\Delta t/2)
\end{aligned} \tag{5}$$

where M is the total number of particles of a given species. The mean local flux vector field was computed by averaging Eqs. 5 over the production MD trajectories.

In Figure 6a, the local fluxes were computed using $l_x = 10.42$ Å, $l_y = 2.02$ Å and $l_z = 7.41$ Å. To visualize the mean 3D flux field using a 2D plot, we averaged the 3D vector field over the y axis. The resulting 2D vector field was converted to streamline plots using the streamplot function of the matplotlib library.[2]

Calculations of the ionic conductivity. Figure S1a illustrates the electric circuit model used to determine the conductivity of a DNA origami plate in z direction ($\sigma_{o,z}$). The total resistance of the

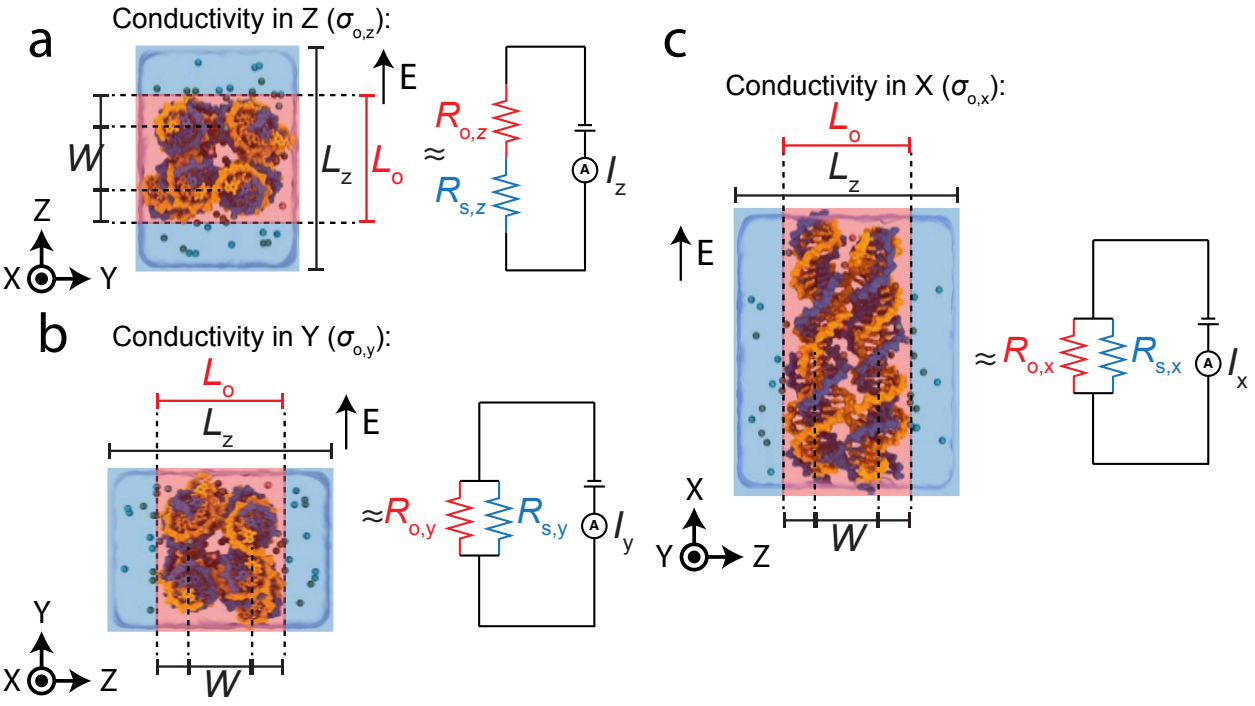

Figure S1: (a) Electric circuit model of the MD simulation of the DNA origami conductivity in z direction ($\sigma_{o,z}$). The all-atom system containing a DNA origami plate and ionic solution is modeled as two resistors connected in series; R_o is the resistance of the origami plate and R_s is the resistance of the solution. During the applied potential simulations, the dimensions of the system L_x, L_y and L_z are fixed. The ionic current is determined by summing up local displacements of all charged species in the system, the applied potential $V = -L_z E$.[1] To compute the conductivity of the DNA origami plate, the plate's extension along the z axis L_o is computed as $W + 2\Delta$, where W is the average distance between the centers of mass of the top and bottom layers of the origami and Δ = 1.5 nm is the extension of the ion atmosphere around a DNA helix.[3] (b, c) Electric circuit model of the MD simulation of the DNA origami conductivity in the y ($\sigma_{o,y}$, panel b) and x ($\sigma_{o,x}$, panel c) directions. In both cases, the systems are modeled as two resistors connected in parallel.

system in z direction

$$R_{\mathrm{t,z}} = R_{\mathrm{o,z}} + R_{\mathrm{s,z}}, \tag{6}$$

where $R_{\mathrm{o,z}}$ and $R_{\mathrm{s,z}}$ are the resistances of the origami plate and solution in z direction, respectively. The resistance of the solution can be calculated as

$$R_{\mathrm{s,z}} = \rho_{\mathrm{s,z}} \frac{L_{\mathrm{s}}}{L_{\mathrm{x}} L_{\mathrm{y}}}, \tag{7}$$

where $\rho_{\mathrm{s,z}}$ is the resistivity of the solution in z direction, L_{x} and L_{y} are the dimensions of the simulation system along the x and y axes, respectively. The thickness of the solution $L_{\mathrm{s}} = L_{\mathrm{z}} - L_{\mathrm{o}}$, where L_{z} and L_{o} are the dimensions of the entire simulation system and of the DNA origami plate, respectively, along the z-axis.

To determine the resistivity of the solution, we built $5.2\times10.4\times10.5$ nm^3 ($\sim$360 mM $MgCl_2$/1M KCl) and a $3.2\times3.2\times3.2$ nm^3 ($\sim$50 mM $MgCl_2$/1M KCl) systems. The systems were first equilibrated for $\sim$48 ns and were then subjected to the applied bias of 100, 250 or 500 mV for 9.6 ns each. The average ionic current was calculated for each system using block-averaged values sampled at 0.96 ns. The resistivity of the solution

$$\rho_{\mathrm{s}} = \frac{V}{I} \times \frac{A}{L}, \tag{8}$$

where V is the bias, I is the current, L is the length of the simulation cell in the direction of the applied electric field (z axis in our simulations) and A is the area of the system normal to the applied field. Obtained resistivities of the two solutions did not depend on the applied bias or on the concentration of Mg^{2+}, Figure S2.

To determine the conductivity of a DNA origami plate, we defined its thickness in the direction of the applied field as $L_{\mathrm{o}} = W + 2\Delta$. For square-lattice origami, W was defined as the distance between the centers of mass of the scaffold strand in the top and bottom layers of the plate. For

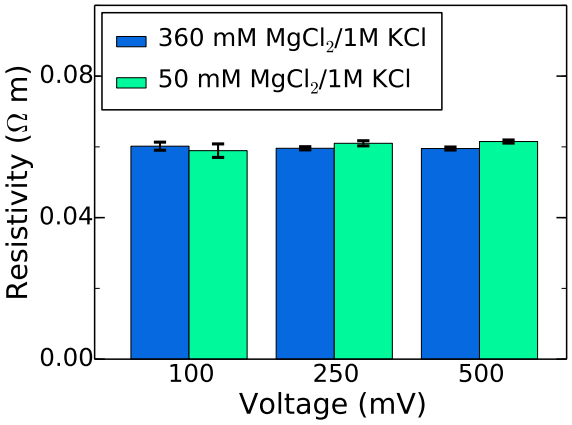

Figure S2: MD simulations of bulk solution resistivity. Each data point was extracted from a 9.6 ns MD trajectory sampled every 2.4 ps. The data was blocked-averaged with a block size of 0.96 ns. The error bars represent the standard error of the mean of the block-averaged data.

the HC2 and HX2* plates, W was the distance between the centers of mass of the scaffold strand in the top (helix 1) and bottom (helix 4) helices, Figure S3c. The extension of the ion atmosphere around DNA Δ was set to 1.5 nm, a typical value for the range of ion concentrations considered in this work.[3]

The conductivity of a DNA origami plate $\sigma_{\mathrm{o,z}} = 1/\rho_{\mathrm{o,z}} = L_{\mathrm{o}}/(L_{\mathrm{x}}L_{\mathrm{y}}) \times 1/(R_{\mathrm{t,z}} - R_{\mathrm{s,z}})$. Using Eq. 7 for $R_{\mathrm{s,z}}$ and V/I_{z} for $R_{\mathrm{t,z}}$, we obtain

$$\sigma_{\mathrm{o,z}} = \frac{< L_{\mathrm{o}} >< I_{\mathrm{z}} >}{V L_{\mathrm{x}} L_{\mathrm{y}} - \rho_{\mathrm{s}} < I_{\mathrm{z}} > (L_{\mathrm{z}} - < L_{\mathrm{o}} >)}. \tag{9}$$

In the above expression, the total ionic current $< I_{\mathrm{z}} >$ in z direction and the length of the DNA origami $< L_{\mathrm{o}} >$ are determined from the MD trajectory; V is the applied bias. To determine $< I_{\mathrm{z}} >$ and $< L_{\mathrm{o}} >$, their instantaneous values $I_{\mathrm{z}}(t)$ and $L_{\mathrm{o}}(t)$ were block-averaged from a 2.4 ps sampled trajectory using a block size of 9.6 ns. The average conductivity and the standard error were computed using the block-averaged data.

In order to calculate DNA origami conductivities in y and x directions, $\sigma_{\mathrm{o,y}}$ and $\sigma_{\mathrm{o,x}}$, the MD systems were modeled as resistors connected in parallel, Figure S1b and c. The total resistance of

each system is

$$R_{\mathrm{t,y}} = \frac{1}{\frac{1}{R_{\mathrm{o,y}}} + \frac{1}{R_{\mathrm{s,y}}}}, \tag{10}$$

$$R_{\mathrm{t,x}} = \frac{1}{\frac{1}{R_{\mathrm{o,x}}} + \frac{1}{R_{\mathrm{s,x}}}}, \tag{11}$$

where $R_{\mathrm{o,y}}$, $R_{\mathrm{o,x}}$, $R_{\mathrm{s,y}}$ and $R_{\mathrm{s,x}}$ are the resistances of the origami plate in y and x direction, and the resistance of the solution in y and x direction, respectively. Based on Eq. 11 and the derivation above, we obtain

$$\sigma_{\mathrm{o,y}} = \frac{< I_{\mathrm{y}} > \rho_{\mathrm{s}} L_{\mathrm{y}} - V L_{\mathrm{x}} (L_{\mathrm{z}} - < L_{\mathrm{o}} >)}{L_{\mathrm{x}} L_{\mathrm{o}} V \rho_{\mathrm{s}}} \tag{12}$$

$$\sigma_{\mathrm{o,x}} = \frac{< I_{\mathrm{x}} > \rho_{\mathrm{s}} L_{\mathrm{x}} - V L_{\mathrm{y}} (L_{\mathrm{z}} - < L_{\mathrm{o}} >)}{L_{\mathrm{y}} L_{\mathrm{o}} V \rho_{\mathrm{s}}} \tag{13}$$

Similarly, $I_{\mathrm{y}}(t)$, $I_{\mathrm{x}}(t)$ and $L_{\mathrm{o}}(t)$ were block-averaged from a 2.4 ps sampled trajectory using a block size of 9.6 ns. The average conductivity and the standard error were computed using the block-averaged data.

Correction to Cuboid X trapping measurements of ΔG. To directly compare the relative conductance blockades produced by Cuboids X and Y, we need to account for the fact that the cuboids were longer (29 nm) in one dimension (along DNA helices) than in the other two (both 23 nm). In order to do so, we estimate what the relative conductance change ($\Delta G'$) of Cuboid X would be if it were to have the same length as Cuboid Y. Assuming that the resistance of a DNA origami object is proportional to its length, the resistance of the length-adjusted Cuboid X, $R'_{\mathrm{x}} = \frac{23}{29} R_{\mathrm{x}}$, where R_{x} is the resistance of the original Cuboid X. Then, the resistance of the hybrid DNA origami/nanocapillary structure, R'_{h}, would be

$$R'_{\mathrm{h}} = R_{\mathrm{c}} + \frac{23}{29} R_{\mathrm{x}}, \tag{14}$$

where R_{c} is the resistance of the bare nanocapillary.

The ionic current measured upon placement of the reduced-length Cuboid X on top of the

nanocapillary I'_{h} would be

$$I'_{\mathrm{h}} = \frac{V}{R'_{\mathrm{h}}} = \frac{V}{\frac{V}{I_{\mathrm{c}}} + \frac{23}{29} \times (\frac{V}{I_{\mathrm{h}}} - \frac{V}{I_{\mathrm{c}}})}, \tag{15}$$

where I_{c} and I_{h} are the ionic currents through the bare nanocapillary and the hybrid structure (before the correction), respectively, at the applied voltage V. The corrected value of the relative conductance change is then

$$\Delta G' = \frac{I_{\mathrm{c}} - I'_{\mathrm{h}}}{I_{\mathrm{c}}}. \tag{16}$$

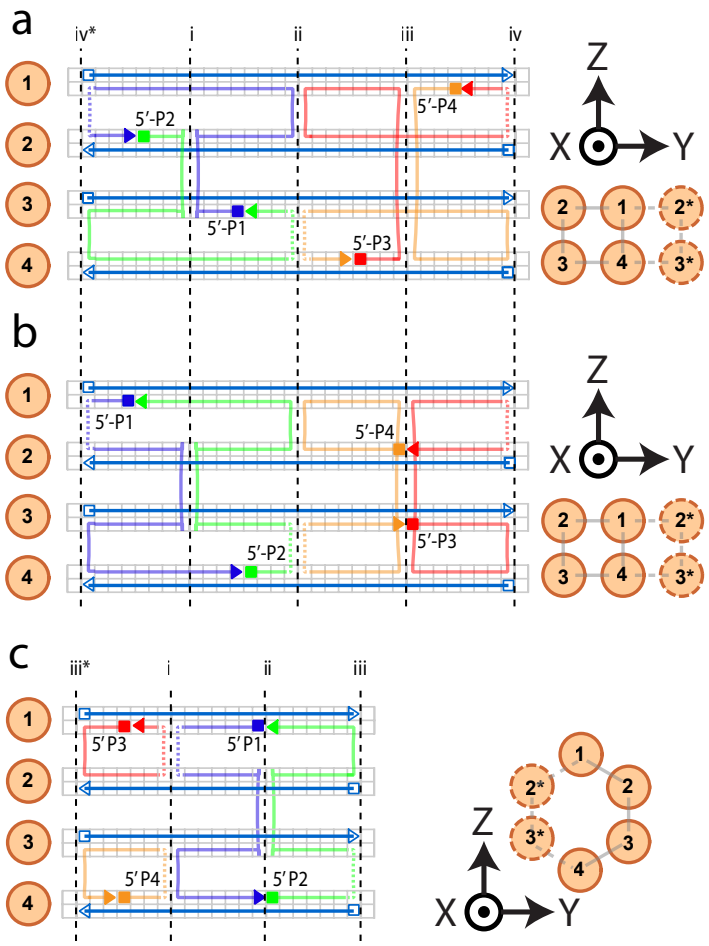

Figure S3: Connectivity map of the SQ2 and HC2 plates. (a) Connectivity map of the m13 SQ2 plate. The left panel shows the connectivity of the unit cell. DNA helices of the plate are labeled using numbers on the left. A gray grid schematically represents each DNA helix; each grid segment corresponds to one DNA base pair (bp). Each helix of the SQ2 plate contains 32 bp per unit cell. Vertical dashed black lines indicate the location of crossover planes. The crossover planes are separated by 8 bp and labeled as i, ii, iii, iv. Under periodic boundary conditions, the plate is effectively infinite in the $x-y$ plane but not along the z axis. Hence, the crossover plane iv* on the left is the periodic mirror image of the crossover plane iv on the right. Horizontal solid blue lines represent the scaffold. The 5' end (open square) and the 3' end (open triangle) of the scaffold fragment are covalently connected across the periodic boundary of the system in each helix. The lines weaving among the DNA helices (multiple colors) represent the staple strands (labeled as P1–P4); the dashed parts of the lines indicate connections across the periodic boundaries of the system. The filled squares and triangles indicate the 5' and 3' ends of the staple strands; Table S2 details their nucleotide sequence. The right panel shows the physical arrangement of the DNA helices. Helices 2* and 3* are the periodic images of helices 2 and 3, respectively. Crossovers in the unit cell and across the periodic boundaries of the system are schematically shown using solid and dashed gray lines, respectively. (b) Connectivity map of the AT/CG-rich SQ2 plates. Apart from the location of the 5' and 3' ends of the staple strands, the map is identical to that of the m13 SQ2 plate (panel a). Table S2 details the nucleotide sequences of the staple strands. (c) Connectivity map of the HC2 plate. The map is drawn using the same representations as the map of m13 SQ2, panel a. Each helix of the HC2 plate contains 21 bp per unit cell; the crossover planes are separated by 7 bp. Table S2 details the nucleotide sequences of the staple strands.

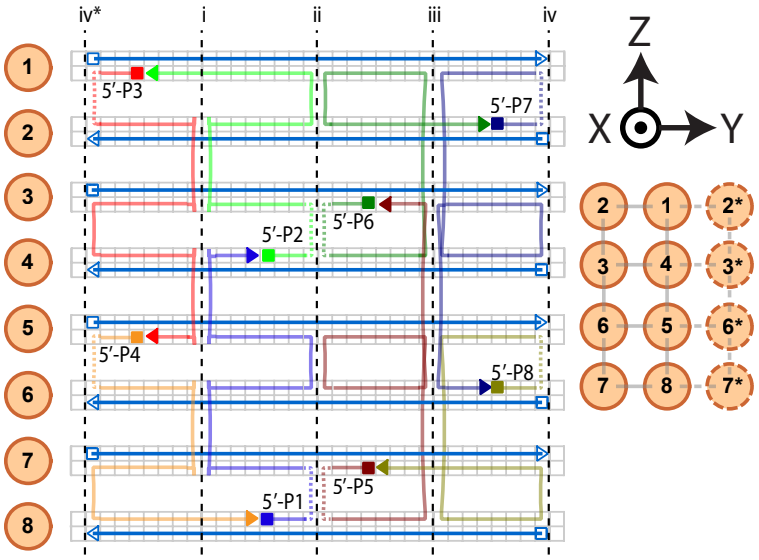

Figure S4: Connectivity map of the SQ4 plate. The map is drawn using the same representations as the map of m13 SQ2, Figure S3a. Staple strands P1, P3, P5 and P7 bridge up to three consecutive layers of the plate. Table S2 details the nucleotide sequences of the staple strands.

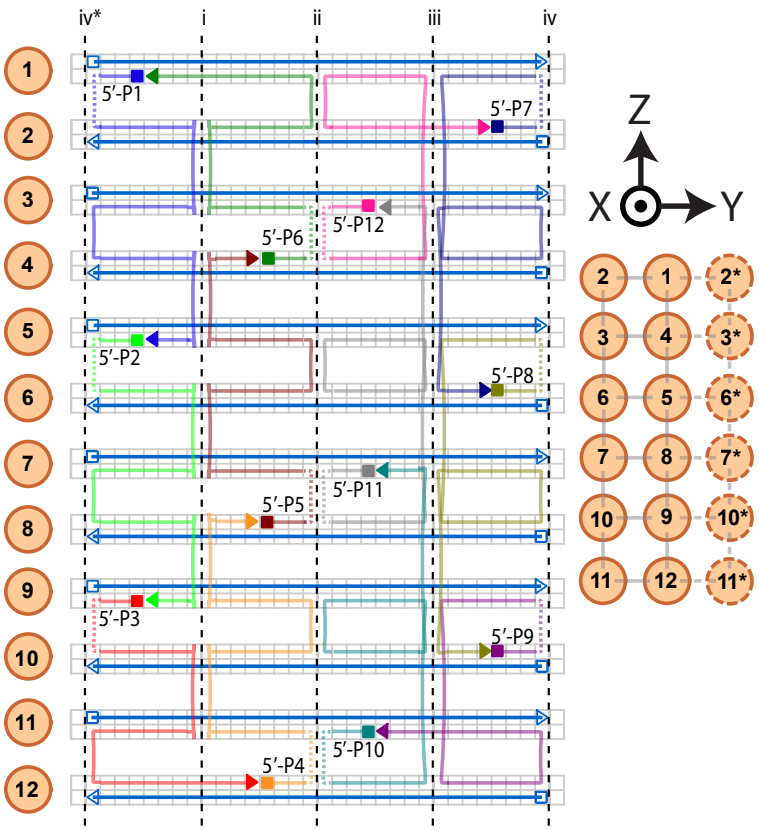

Figure S5: Connectivity map of the SQ6 plate. The map is drawn using the same representations as the map of m13 SQ2, Figure S3a. Staple strands P1, P2, P4, P5, P7, P8, P10 and P11 bridge up to three consecutive layers. Table S2 details the nucleotide sequences of the staple strands.

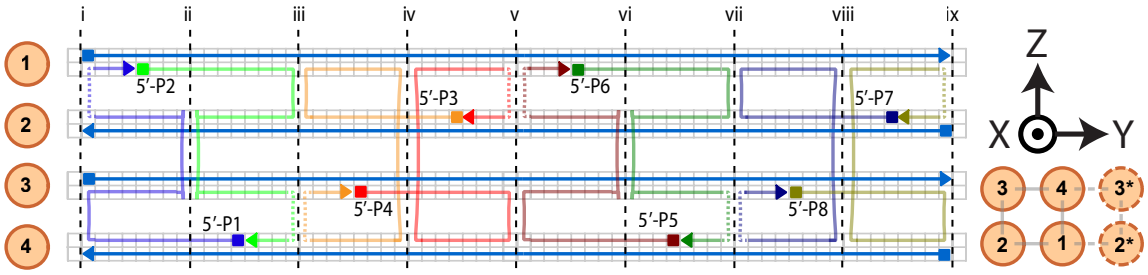

Figure S6: Connectivity map of the SQ2 hybrid origami. The map is drawn using the same representations as the map of m13 SQ2, Figure S3a. Filled blue squares and triangles indicate the 5' and 3' ends of the scaffold strand, respectively, that are not covalently bonded to each other across the periodic boundary of the system. Table S2 details the nucleotide sequences of the staple strands.

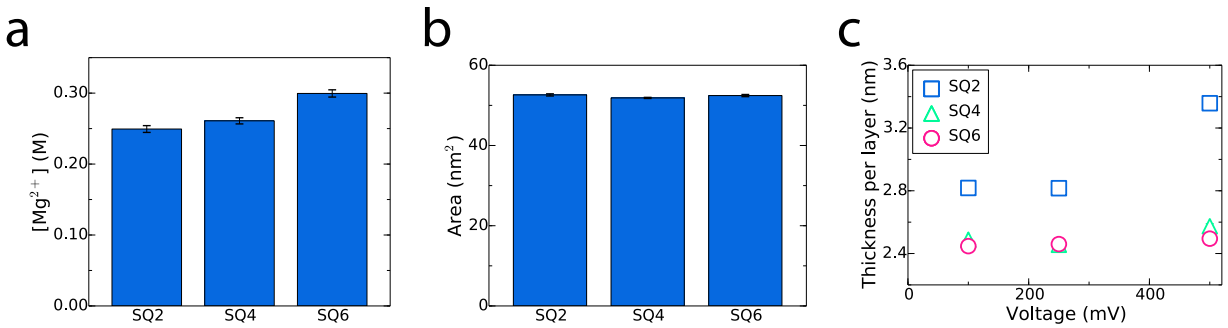

Figure S7: MD simulations of ion transport through SQ2, SQ4 and SQ6 plates. (a) Bulk concentration of Mg^{2+} in the simulations of the SQ2, SQ4 and SQ6 systems. (b) Cross section area L_xL_y of the SQ2, SQ4 and SQ6 systems. (c) Thickness per layer of the DNA origami plates.

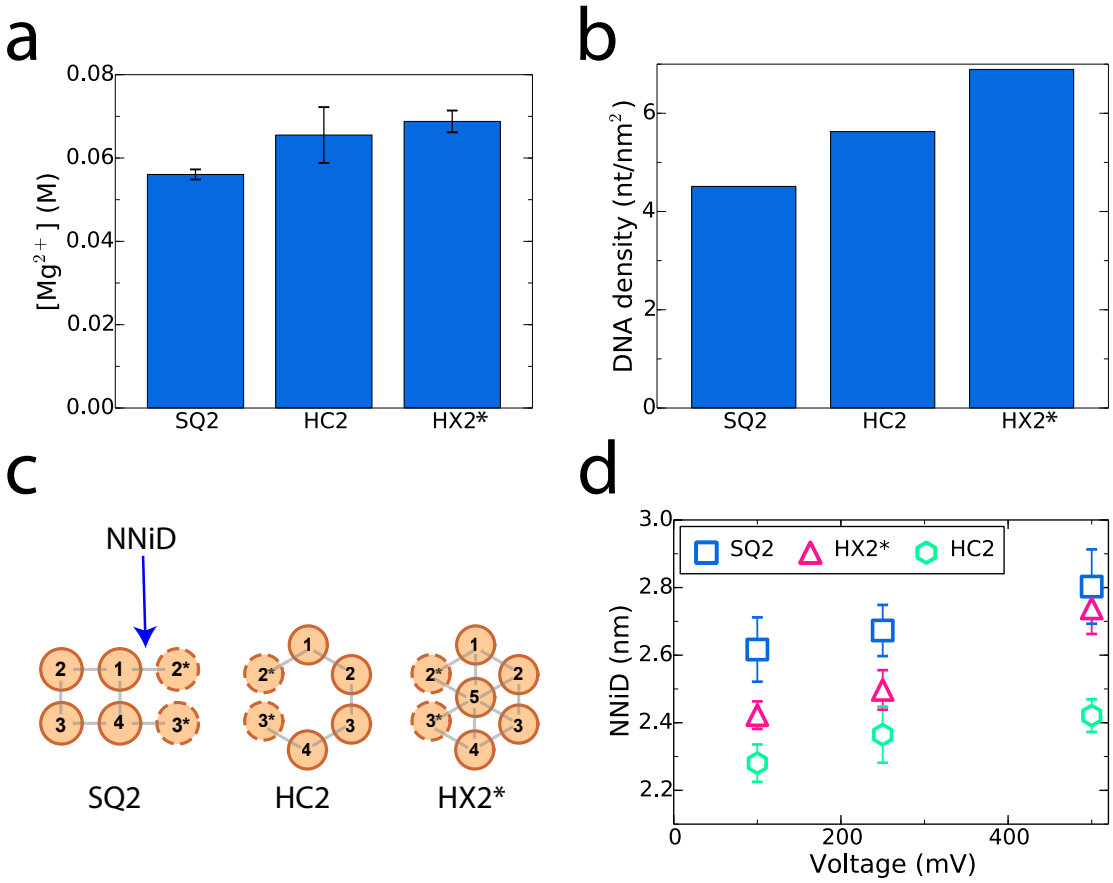

Figure S8: MD simulations of ion transport through SQ2, HC2 and HX2* plates. (a) Bulk concentration of Mg^{2+} in the simulations of the SQ2, HC2 and HX2* systems. (b) Density of the DNA origami plates projected onto the $x-y$ plane. (c) Definition of the nearest-neighbor inter-DNA (NNiD) distance. The NNiD distance was defined as the distance between the centers of the nearest-neighbor DNA helices. For clarity, periodic images of helices 2 and 3 (helices 2* and 3*) are shown. The NNiD distance was computed over 6 (SQ2), 5 (HC2) and 11(HX2*) unique distance pairs of the corresponding unit cell. (d) The voltage dependence of the NNiD distance. Each symbol represents an average over a 48 ns trajectory sampled every 2.4 ps. The error bars show the standard error of the mean.

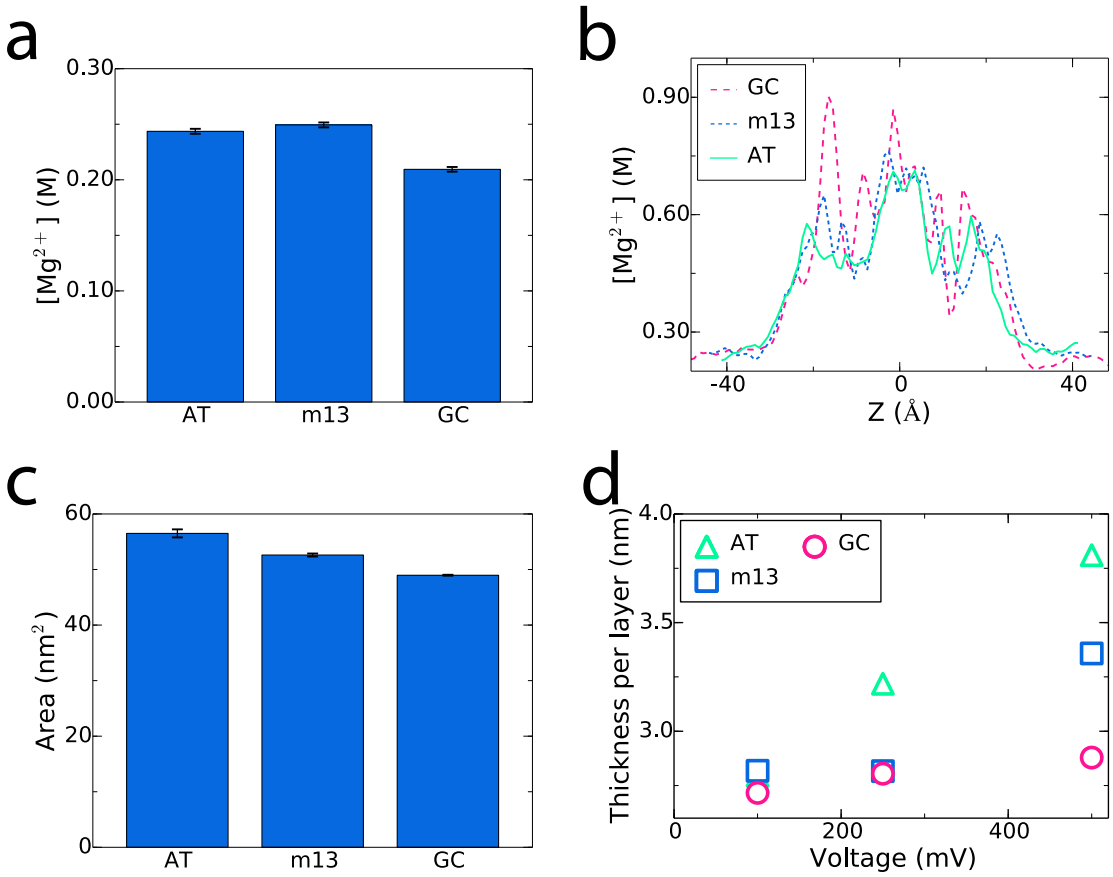

Figure S9: MD simulations of ion transport through AT,- CG- and m13-sequence SQ2 plates. (a) Bulk concentration of Mg^{2+} in the simulations of the AT, CG and m13 systems. The three systems contain the same number of K^+, Cl^-, Mg^{2+} ions and the same number of water molecules. (b) Average profile of Mg^{2+}concentration across the AT-, CG- and m13-sequence plates. In each system, the center of mass of the origami is at $z = 0$. (c) Equilibrium cross section area (L_xL_y) of the AT, CG and m13 systems. Each data point was obtained by averaging the last 400 ns fragment of the corresponding equilibration trajectory sampled every 2.4 ps. (d) Thickness per layer of the DNA origami in the AT, CG and m13 systems. Each data point represents an average from a 48 ns trajectory.

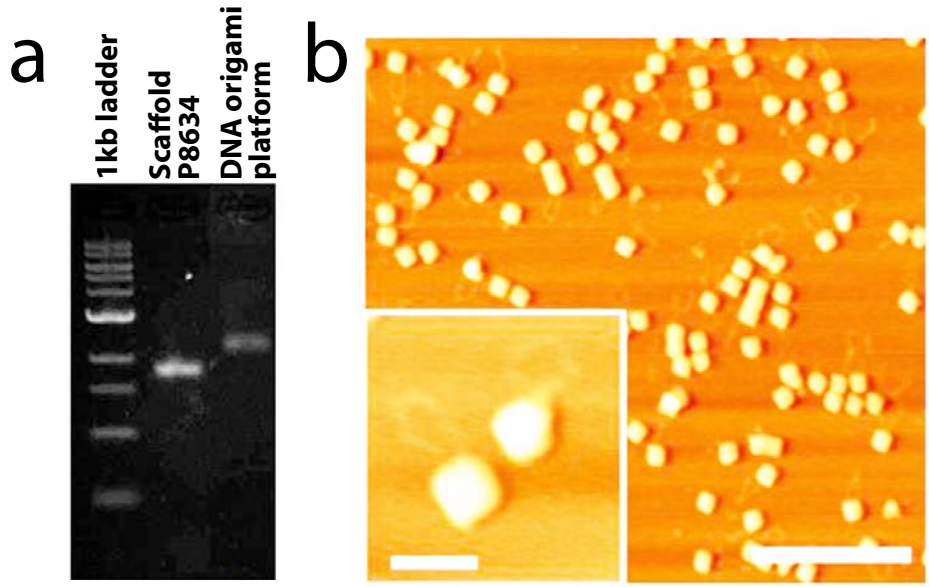

Figure S10: (a) Agarose gel (1%) electrophoresis of the DNA origami platforms, which was performed in 11 mM $MgCl_2$ buffered in 0.5$\times$ TBE. A single band indicates successfully folded structures. (b) Atomic force microscopy images of individual DNA origami platforms. The scale bar corresponds to 100 (inset) and 600 (main figure) nm.

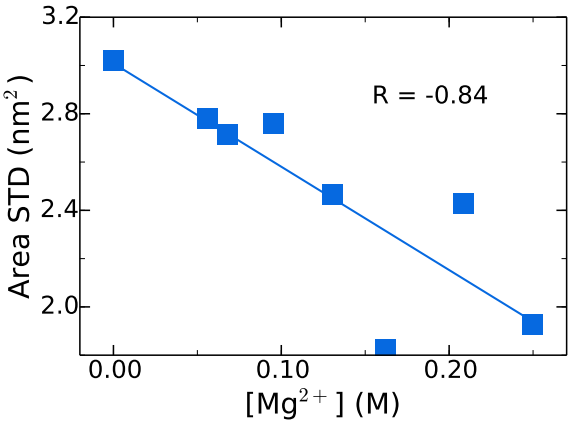

Figure S11: Magnesium dependence of area fluctuation in MD simulations of the m13 SQ2 systems. Standard deviation (STD) of the area is plotted *versus* bulk concentration of Mg^{2+}. The line shows a linear fit to the data; R is the Pearson's correlation coefficient of the fit. Each data point was obtained from the last 400 ns fragment of the corresponding equilibration trajectory sampled every 2.4 ps.

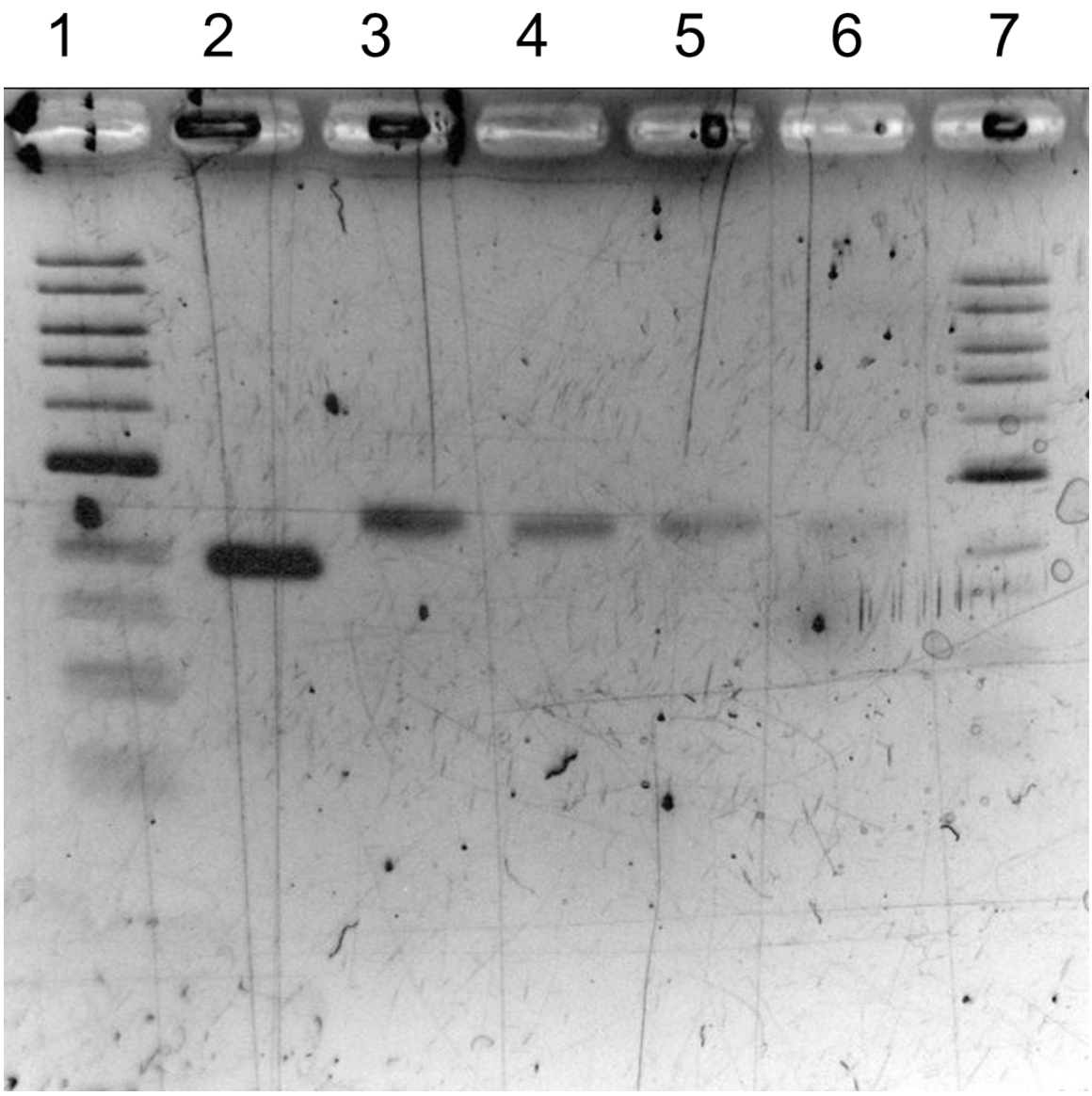

Figure S12: Agarose gel (1%) electrophoresis of the fluorescently labeled DNA origami platforms performed in 11 mM $MgCl_2$ buffered in 0.5×TBE. Lane 1 and 7 show a 1 kb DNA ladder; lane 2: 8634 scaffold; lane 3: unmodified DNA origami platform; lane 4: DNA origami platform, parallel arrangement of the dyes; lane 5: DNA origami platform, perpendicular arrangement of the dyes; lane 6: DNA origami platform, diagonal arrangement of the dyes. Single bands in lanes 4–6 appear at the same location as in the case of unmodified DNA origami structures (lane 3), which indicates the correct assembly of the fluorescently labeled DNA origami structures.

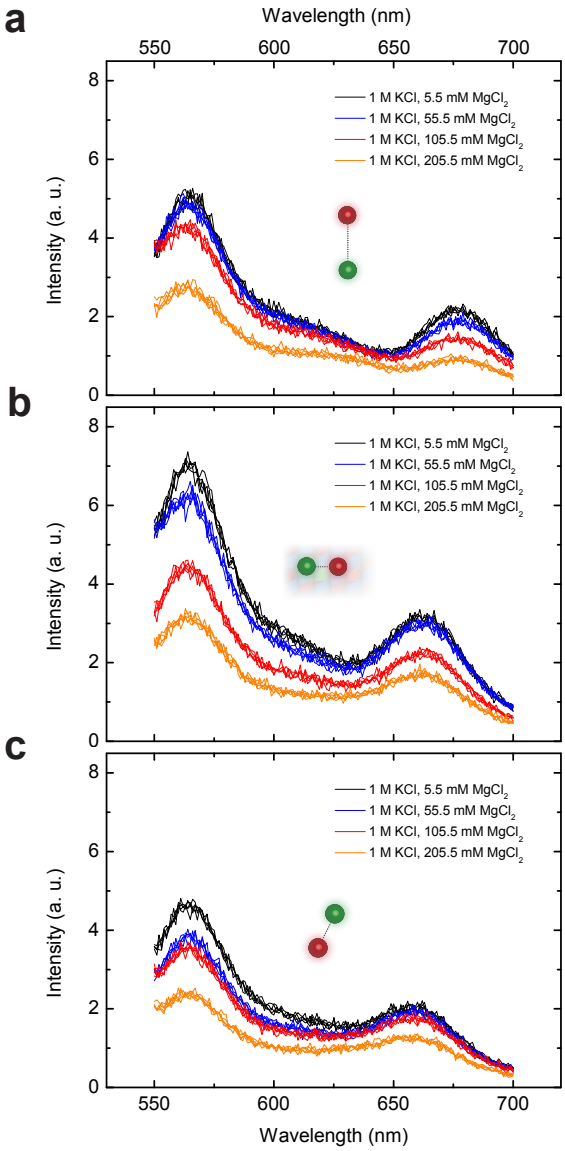

Figure S13: Emission spectra of fluorescently labeled DNA origami. Data in panels a, b and c correspond to the parallel, perpendicular and diagonal arrangements of the dyes with respect to the DNA helix direction. Measurements were performed at 1 M KCl, 0.5× TBE and $MgCl_2$ concentrations of 5.5 (black), 55.5 (blue), 105.5 (red), 205.5 (orange) mM. The samples were excited at a wavelength of 521 nm, the excitation slit was 20 nm. For all three designs, the overall emission intensity decreased as the concentration of $MgCl_2$ was increased. Dilution of the DNA origami sample could only partially explain this effect, because the concentration of the DNA origami sample was reduced by a maximum of $\sim$20% as the concentration of $MgCl_2$ increased from 5.5 to 205.5 mM. To determine FRET efficiency E^* as $I_A/(I_D + I_A)$, the intensity profiles were integrated within a 550–600 (I_D) and 650–700 (I_A) nm range. These integration windows were chosen such that the contribution of Cy3 emission to the Cy5 intensity peak was minimal and that the calculated intensities corresponded to isolated parts of the spectrum.

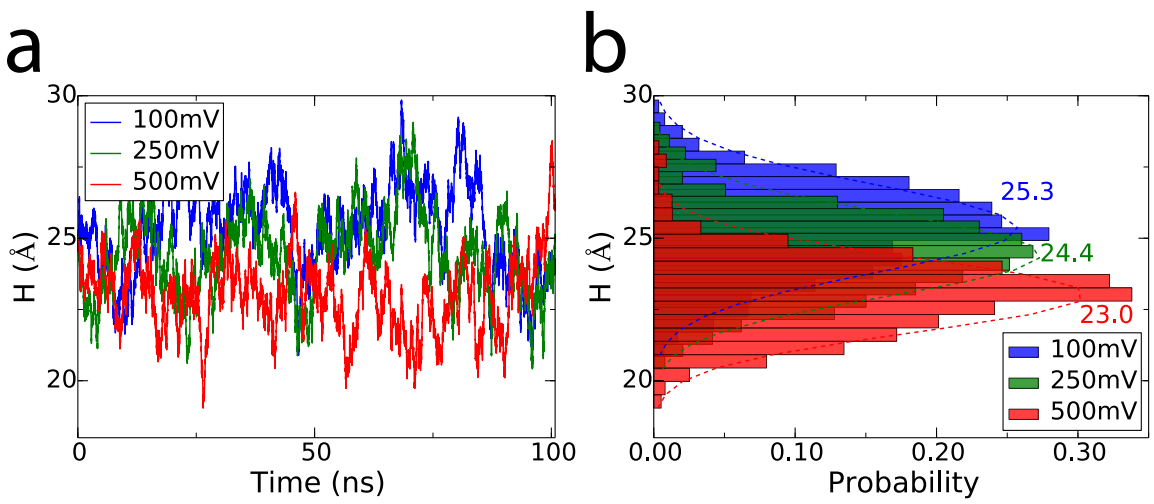

Figure S14: Voltage-dependent deformation of the SQ2/SiO_2 hybrid system. (a) The distance between the center of mass of the SQ2 plate and the surface of the SiO_2 support structure, H, *versus* the simulation time at applied bias of 100, 250, and 500 mV. (b) Histograms of the traces shown in panel a.

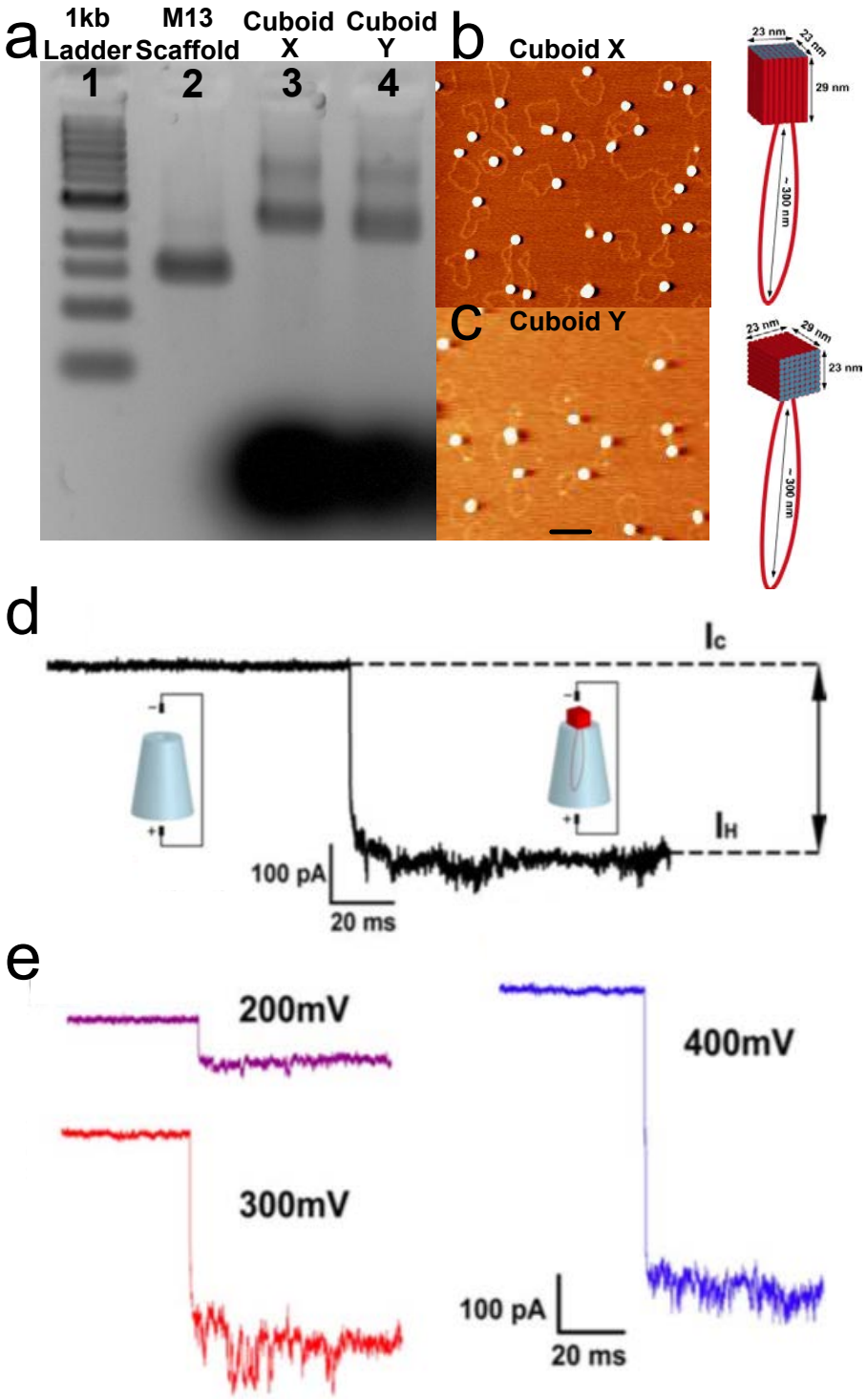

Figure S15: Characterization of cuboid-shaped DNA origami. (a) Electrophoresis gel image of origami Cuboid X and Cuboid Y. Lane 1: 1kb DNA ladders; Lane 2: 7249 nt-long scaffold; Lane 3: origami Cuboid X; Lane 4: origami Cuboid Y. (b, c) AFM images of origami Cuboid X and Cuboid Y. The scale bar is 500 nm. The cuboid and the attached guiding leash can be clearly seen in most of the structures. (d) A typical ionic current trace showing the capture of a DNA origami cuboid. The drop of the ionic current indicates the presence of a DNA origami cuboid at the tip of a nanocapillary. The schematic images illustrate the trapping process. (e) Example traces of origami Cuboid Y trapping at 200 mV (purple), 300 mV (red) and 400 mV (blue) in 1 M KCl, 5 mM $MgCl_2$, 0.5×TBE and pH 8.3.

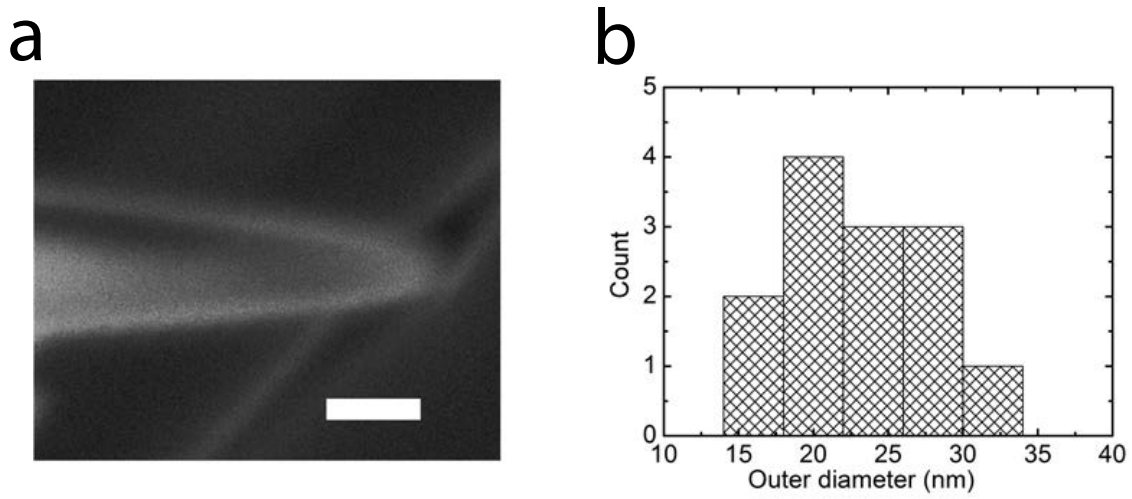

Figure S16: (a) Scanning electron microscopy (SEM) image showing the conical shape of a glass nanocapillary. Scale bar = 50 nm. (b) Histogram of the outer diameter of 13 nanopores observed by SEM images. An outer diameter of mean 22.7 nm and standard deviation 4.9 nm was measured. To estimate the inner wall geometry, we make the approximation that the ratio of outer diameter (OD) to inner diameter (ID) of the capillary is maintained from its initial value all the way to the tip. The initial outer diameter is 0.5 mm, while the initial inner diameter is 0.2 mm. Therefore, the estimated inner diameter after pulling is 9.1 ± 2.0 nm.

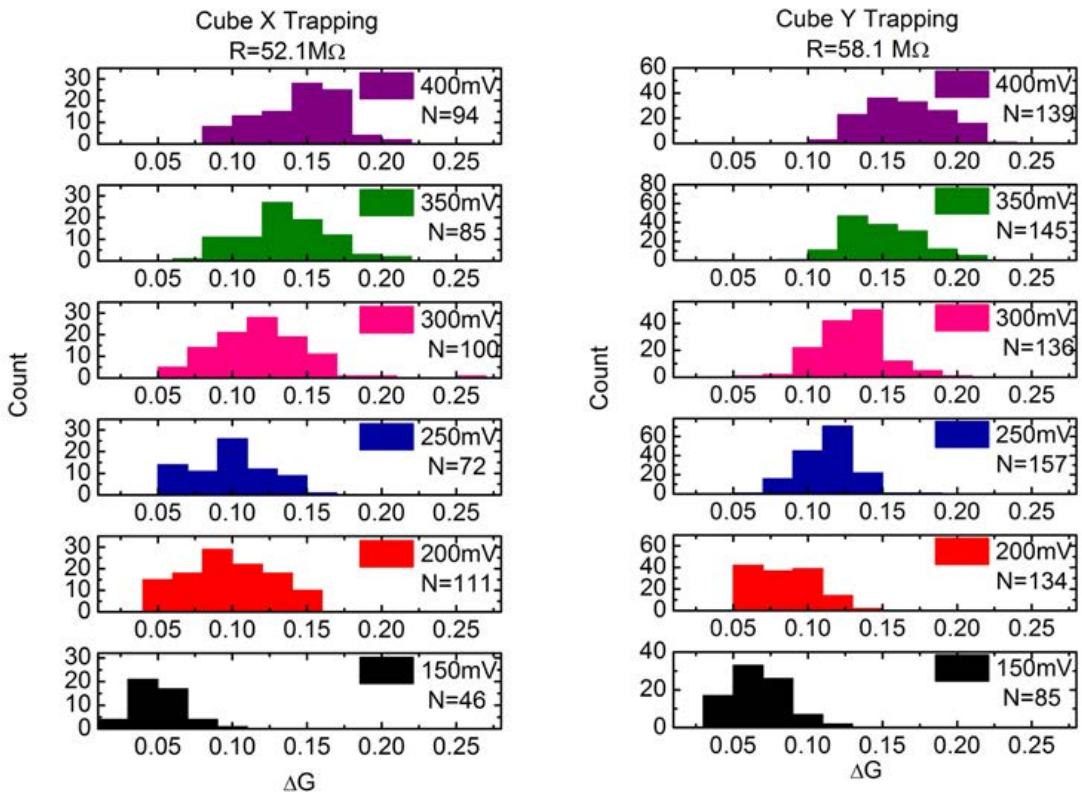

Figure S17: Example histograms of ΔG produced by origami cuboid trapping at different voltages. The resistances of the nanocapillaries are approximately 50 MΩ.

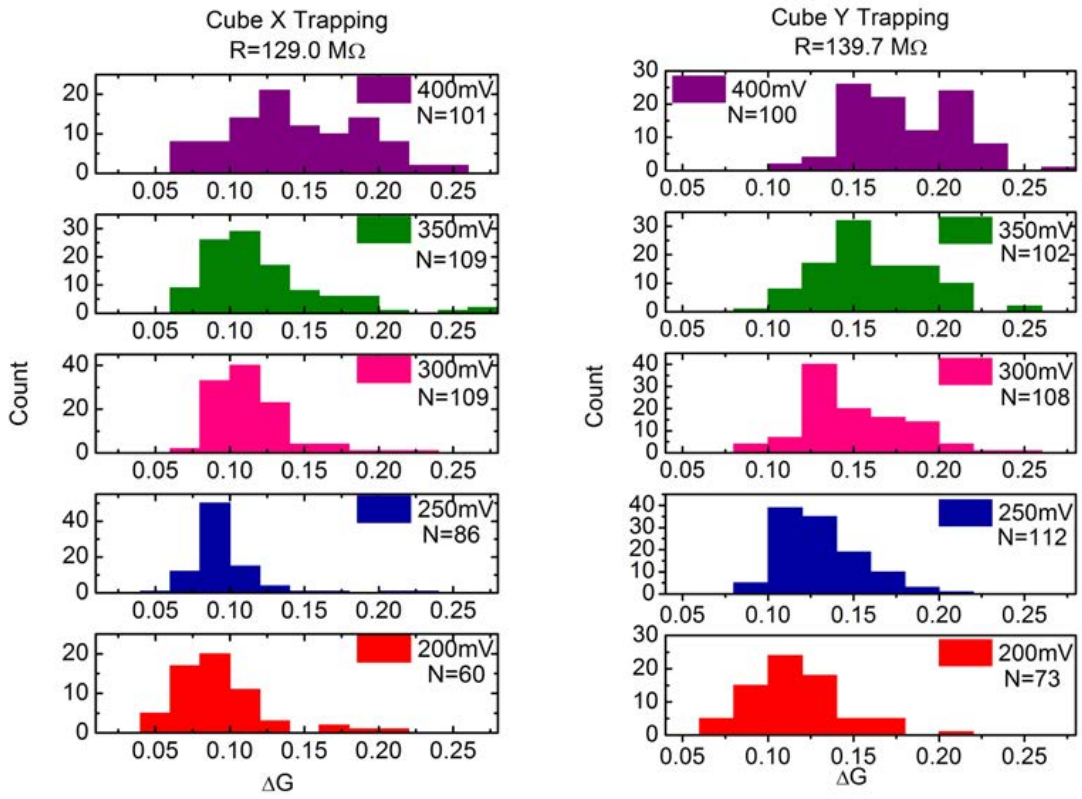

Figure S18: Example histograms of ΔG produced by origami cuboid trapping at different voltages. The resistances of the nanocapillaries are approximately 130 MΩ.

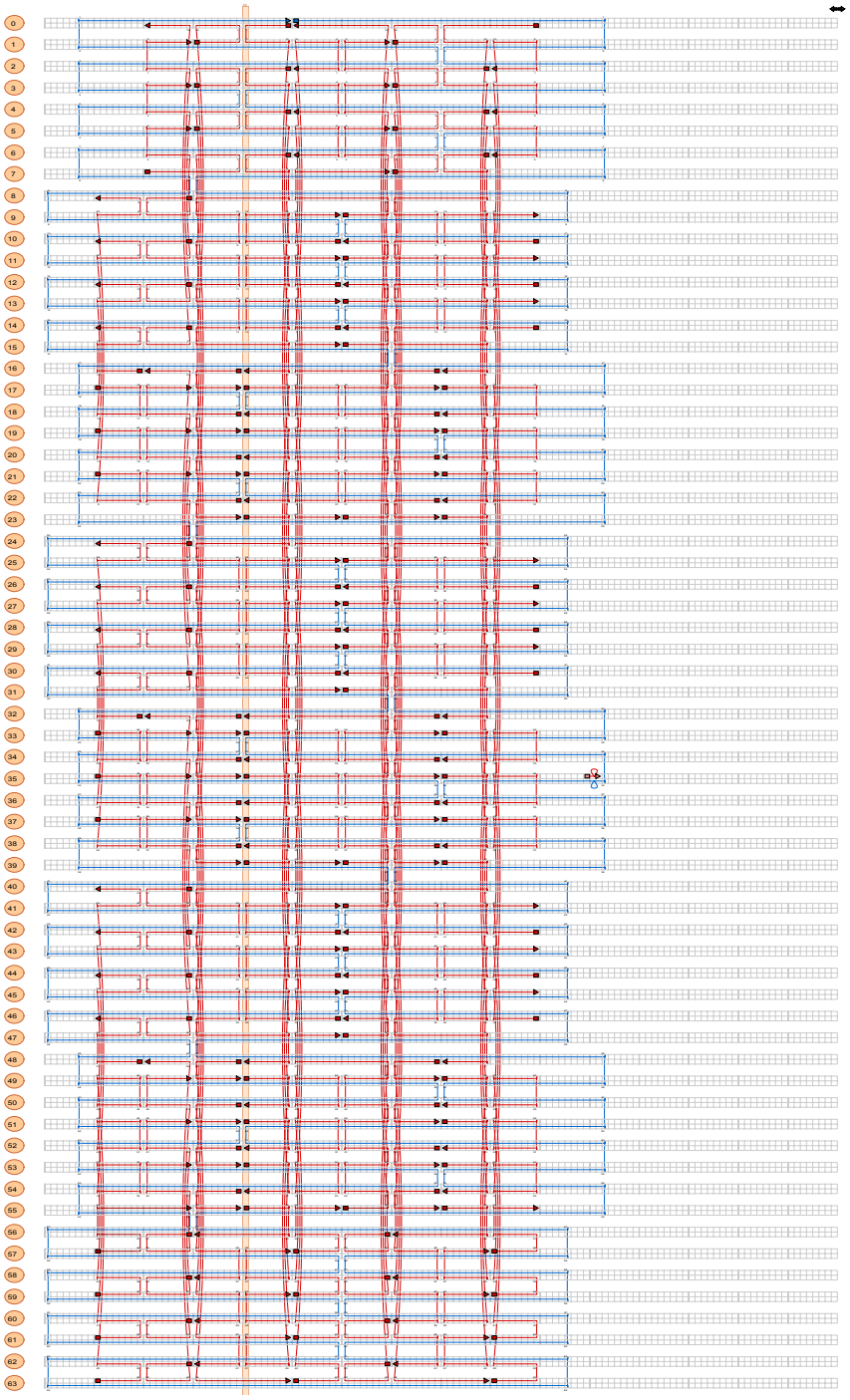

Figure S19: 2D scaffold-staple layout of origami Cuboid X.

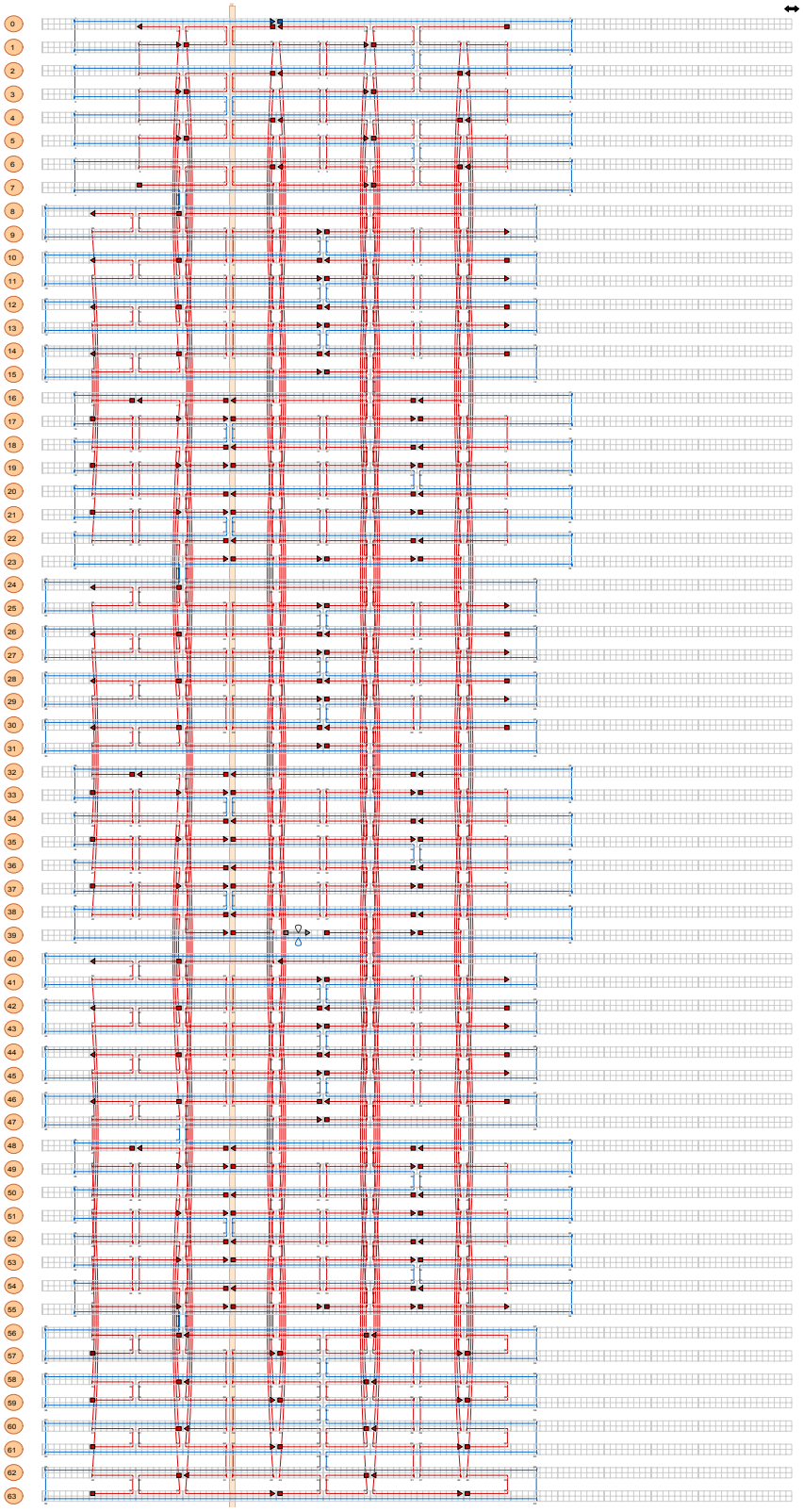

Figure S20: 2D scaffold-staple layout of origami Cuboid Y.

Animations of MD trajectories

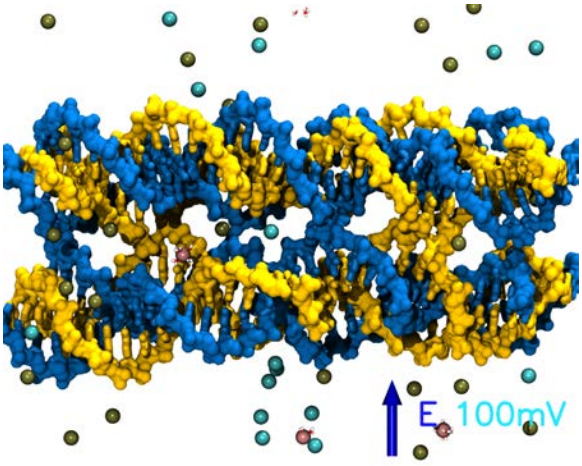

Animation M1: Ionic current through DNA origami. The scaffold and staple strands of the m13 SQ2 origami plate are shown in blue and yellow, respectively; Mg^{2+}, $Cl^{-}$and K^{+}ions are shown as pink, cyan and ochre spheres, respectively. Water molecules forming magnesium hexahydrate complexes with Mg^{2+} are explicitly shown in red (oxygen) and white (hydrogen). The movie illustrates a 48 ns MD trajectory of the system at a 100 mV applied potential and 1 M/$\sim$50 mM bulk concentration of KCl/$MgCl_2$.

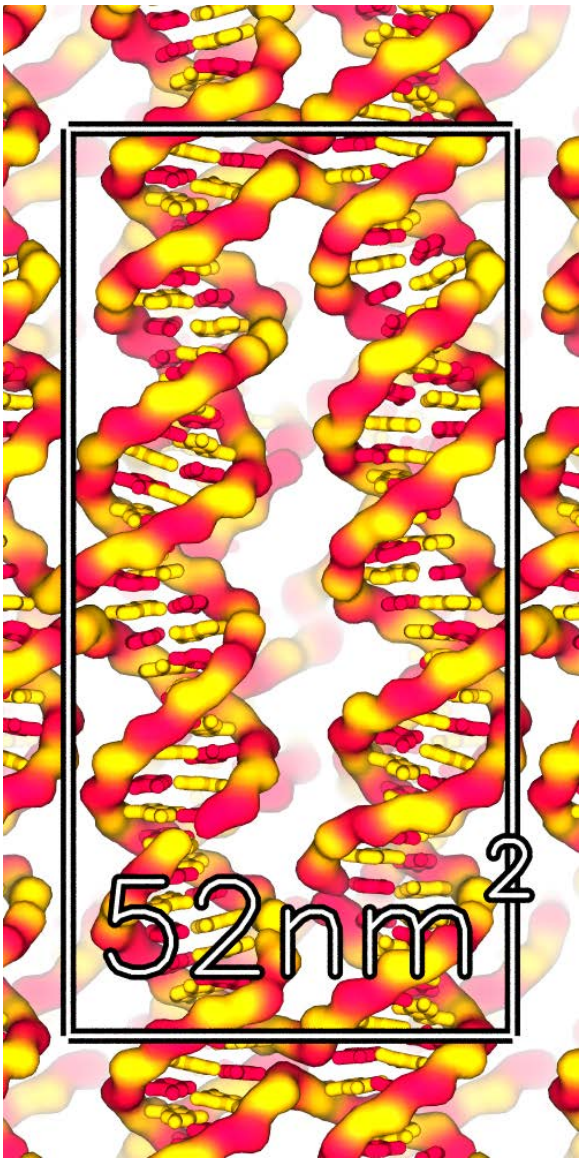

Animation M2: Structural dynamics and cross section area fluctuation of the CG SQ2 plate. Cytosine and guanine nucleotides of the plate are shown in red and yellow, respectively; water and ions are not shown. Several periodic images of the cell are shown. The rectangular box indicates the boundary of the unit cell; the instantaneous area is reported in units of nm^2. The movie illustrates a 573 ns equilibration (zero applied bias) of the system at 1 M KCl /$\sim$250 mM $MgCl_2$ bulk ion concentration.

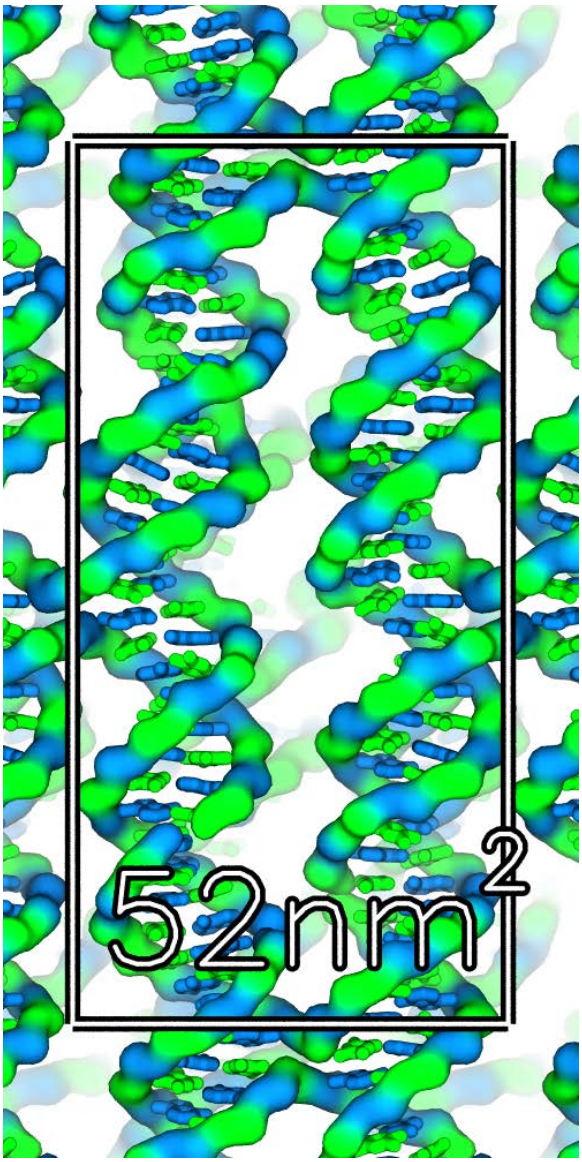

Animation M3: Structural dynamics and cross section area fluctuation of the AT SQ2 plate. Adenine and thymine nucleotides of the plate are shown in blue and green, respectively; water and ions are not shown. Several periodic images of the cell are shown. The rectangular box indicates the boundary of the unit cell; the instantaneous area is reported in units of nm^2. The movie illustrates a 947 ns equilibration (zero applied bias) of the system at 1 M KCl /$\sim$250 mM $MgCl_2$ bulk ion concentration.

Animation M4: Structural dynamics and cross section area fluctuation of the m13 SQ2 plate at high Mg^{2+} concentration. Adenine, thymine, cytosine and guanine nucleotides of the plate are shown in blue, green, red and yellow, respectively; water and ions are not shown. Several periodic images of the cell are shown. The rectangular box indicates the boundary of the unit cell; the instantaneous area is reported in units of nm^2. The movie illustrates a 573 ns equilibration (zero applied bias) of the system at 1 M KCl /$\sim$250 mM $MgCl_2$ bulk ion concentration.

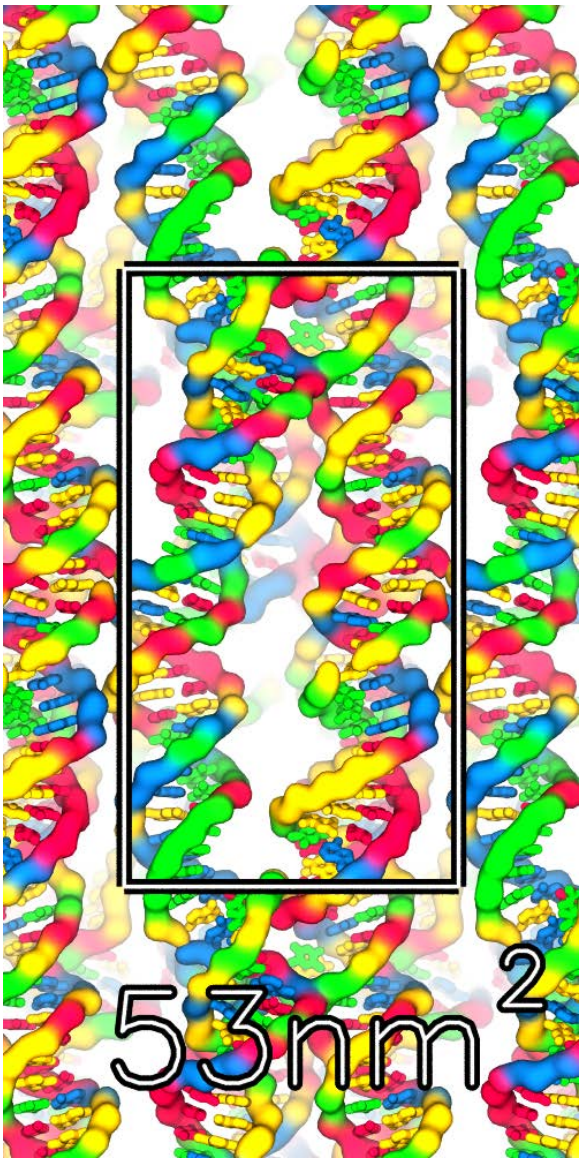

Animation M5: Structural dynamics and cross section area fluctuation of the m13 SQ2 plate at intermediate Mg^{2+} concentration. Adenine, thymine, cytosine and guanine nucleotides of the plate are shown in blue, green, red and yellow, respectively; water and ions are not shown. Several periodic images of the cell are shown. The rectangular box indicates the boundary of the unit cell; the instantaneous area is reported in units of nm^2. The movie illustrates a 654 ns equilibration (zero applied bias) of the system at 1 M KCl /$\sim$131 mM $MgCl_2$ bulk ion concentration.

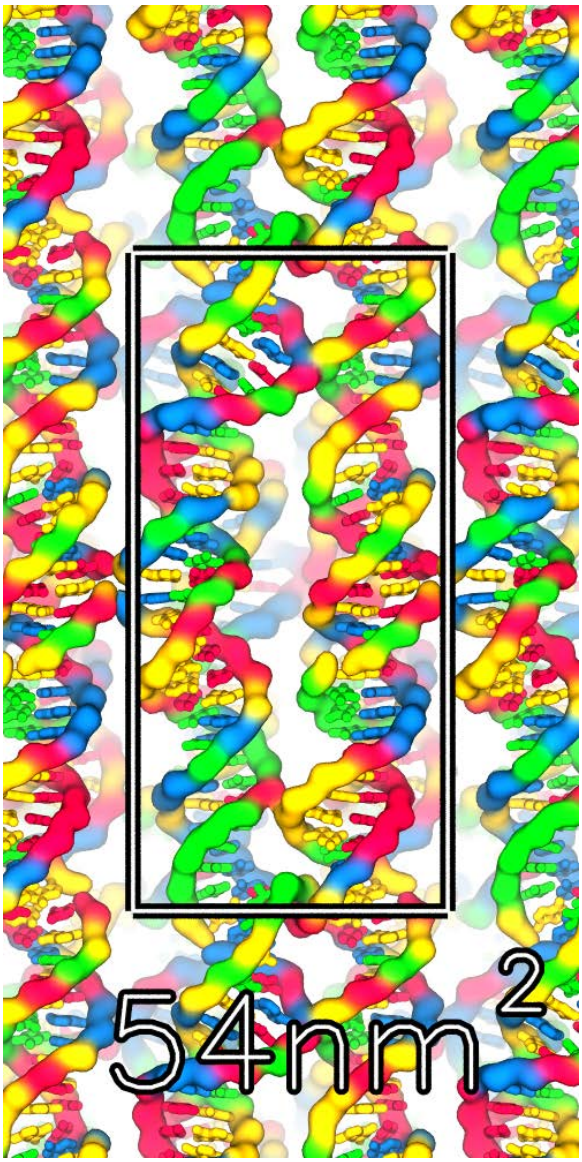

Animation M6: Structural dynamics and cross section area fluctuation of the m13 SQ2 plate at zero Mg^{2+} concentration. Adenine, thymine, cytosine and guanine nucleotides of the plate are shown in blue, green, red and yellow, respectively; water and ions are not shown. Several periodic images of the cell are shown. The rectangular box indicates the boundary of the unit cell; the instantaneous area is reported in units of nm^2. The movie illustrates a 578 ns equilibration (zero applied bias) of the system at 1 M KCl / 0 mM $MgCl_2$ bulk ion concentration.

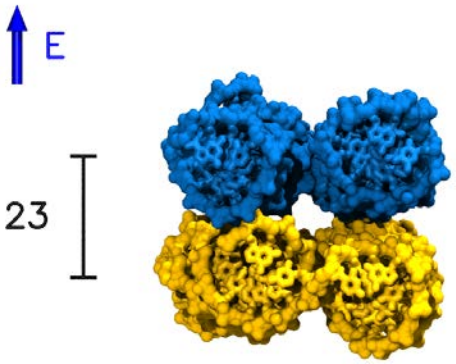

Animation M7: Reversible deformation of a SQ2 plate by electric field. The two layers of the plate are shown in yellow and blue. The arrow indicates application of external electric field corresponding to a 500 mV bias. The instantaneous distance between the scaffold strand in the top and bottom layers of the plate is reported in units of Å. The movie illustrates a 230 ns trajectory of the system at 1 M/∼250 mM bulk concentration of KCl/$MgCl_2$ featured in Figure 5c of the main text.

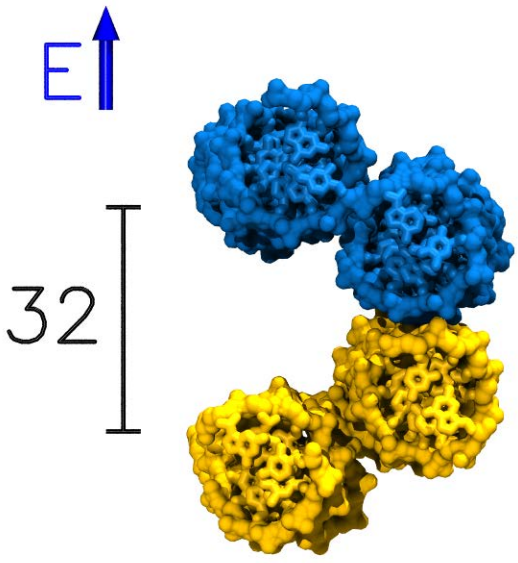

Animation M8: Expansion of a HC2 plate induced by electric field. The top and bottom layers of the structure are shown in blue and yellow, respectively. The instantaneous distance between the scaffold strand in the top and bottom layers of the plate is reported in units of Å. The movie illustrates a 48 ns MD trajectory of the system at a 500 mV applied potential and 1 M/∼50 mM bulk concentration of KCl/$MgCl_2$.

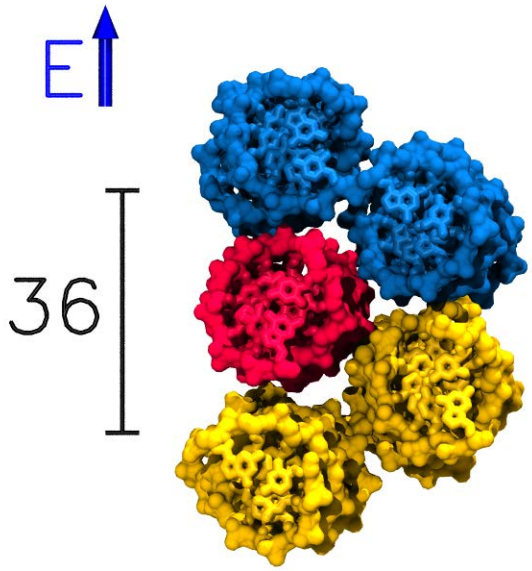

Animation M9: Expansion of a HX2 plate induced by electric field. The top and bottom layers of the structure are shown in blue and yellow, respectively; the center helix, which is not connected to surrounding helices, is shown in red. The instantaneous distance between the scaffold strand in the top and bottom layers of the plate is reported in units of Å. The movie illustrates a 48 ns MD trajectory of the system at a 500 mV applied potential and 1 M/∼50 mM bulk concentration of KCl/$MgCl_2$.

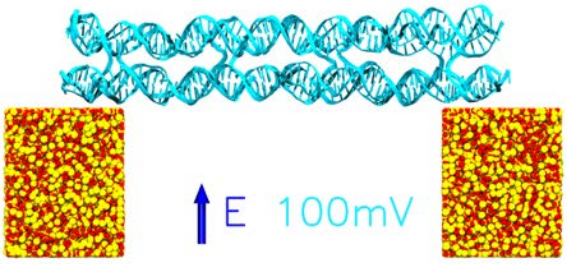

Animation M10: Electric field induced deformation of a DNA origami plate on top of a SiO_2 nanogap. The DNA origami is shown using cyan lines, SiO_2 as red (O) and yellow (Si) spheres; water and ions are not shown. The movie illustrates a 101 ns MD trajectory of the system at a 100 mV applied potential and 1 M/∼50 mM bulk concentration of KCl/$MgCl_2$.

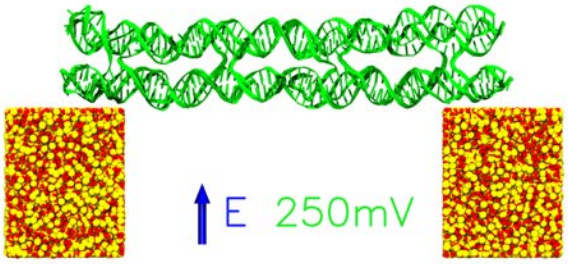

Animation M11: Electric field induced deformation of a DNA origami plate on top of a SiO_2 nanogap. The DNA origami is shown using green lines, SiO_2 as red (O) and yellow (Si) spheres; water and ions are not shown. The movie illustrates a 101 ns MD trajectory of the system at a 250 mV applied potential and 1 M/$\sim$50 mM bulk concentration of KCl/$MgCl_2$.

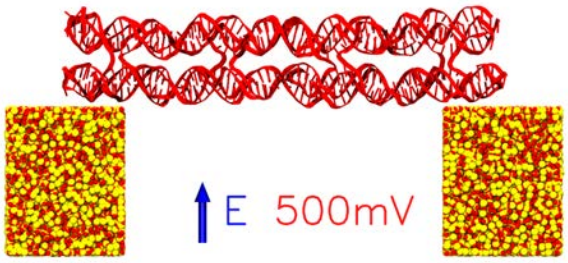

Animation M12: Electric field induced deformation of a DNA origami plate on top of a SiO_2 nanogap. The DNA origami is shown using red lines, SiO_2 as red (O) and yellow (Si) spheres; water and ions are not shown. The movie illustrates a 101 ns MD trajectory of the system at a 500 mV applied potential and 1 M/$\sim$50 mM bulk concentration of KCl/$MgCl_2$.

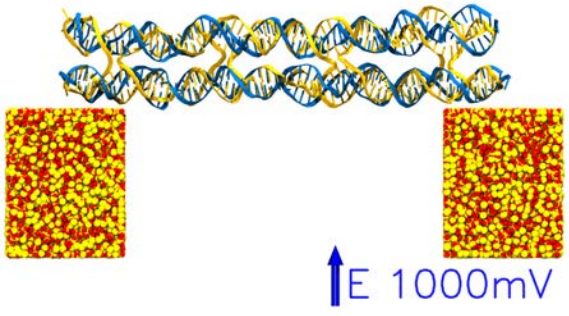

Animation M13: Electric field induced deformation of a DNA origami plate on top of a SiO_2 nanogap. The scaffold and staple strands of the origami are shown as blue and yellow lines, respectively. SiO_2 is shown as red (O) and yellow (Si) spheres; water and ions are not shown. The movie illustrates a 34 ns MD trajectory of the system at a 1000 mV applied potential and 1 M/$\sim$50 mM bulk concentration of KCl/$MgCl_2$.

Supporting Tables

Table S1: Summary of production simulations

	Length (bp) × (# helices)	Sequence[a]	[$MgCl_2$] (mM)	Simulation time (ns)				
				Equilibration[b]	Applied bias simulation[c]			
					0.1	0.25	0.5	1(V)
SQ2	32×(2×2)	AT	∼250	∼950	48	48	48	0
	32×(2×2)	GC	∼250	∼570	48	48	48	0
	32×(2×2)	m13mp18	0	∼580	48	48	48	0
	32×(2×2)	m13mp18	∼50	∼490	48	48	48	0
	Same, electric field applied in *x* direction				48	48	48	0
	Same, electric field applied in *y* direction				48	48	48	0
	32×(2×2)	m13mp18	∼68	∼620	48	48	48	0
	32×(2×2)	m13mp18	∼95	∼610	48	48	48	0
	32×(2×2)	m13mp18	∼131	∼800	48	48	48	0
	32×(2×2)	m13mp18	∼162	∼630	48	48	48	0
	32×(2×2)	m13mp18	∼209	∼630	48	48	48	0
	32×(2×2)	m13mp18	∼250	∼570	48	48	230.4[d]	0
SQ4	32×(2×4)	m13mp18	∼250	∼740	48	48	48	0
SQ6	32×(2×6)	m13mp18	∼250	∼1100	48	48	48	0
HC2	21×(4)	m13mp18	∼50	∼700	48	48	48	0
HX2*	21×(5)	m13mp18	∼50	∼600	48	48	48	0
SQ2 hybrid	64×(2×2)	m13mp18	∼50	∼10	100.8	100.8	100.8	48

[a] The exact sequences are listed in Table S2

[b] Number of atom (N), pressure (P) and temperature (T) are constant.

[c] Number of atom (N), volume (V) and temperature (T) are constant. Electric fields are applied.

[d] The electric field was turned on and off at a 57.6 ns interval, Figure 5c.

Table S2: The nucleotide sequence of staple strands in the all-atom models of DNA origami plates

		Number	Sequence
SQ2	m13	1	GGGTTCCGCTCACCGCTTTCCAGTCGGGAATT
		2	GTTATGAGTGTTGCAGCAAGCGGTCCACGATA
		3	GTTTCTCACTGCCAATTCCACACAACATGCGT
		4	TGCGGCCCCAGCCAAAAGAATAGCCCGAGCTG
	AT	1	TATATATATAATATATATATATATATATATAA
		2	TATATATATATTATATATATATATATATATAT
		3	ATAATATATATATATTATATATATATATATAT
		4	ATATTATATATATAATATATATATATATATAT
	GC	1	CGCGCGCGCGGCGCGCGCGCGCGCGCGCGG
		2	CGCGCGCGCGCCGCGCGCGCGCGCGCGCGC
		3	GCGGCGCGCGCGCGCCGCGCGCGCGCGCGC
		4	GCGCCGCGCGCGCGGCGCGCGCGCGCGCGC
SQ4		1	TCACCTGAGAGAAAGCGCCAGCTATTACCTGG
		2	AGCAAATCATATTAGATTTATCATTTGGGGCG
		3	CGAGCGAACGAGGTACCCCGCTGAGAGTGCCA
		4	GCTGACCAGGCAGTTGCAGCTGGTTTTTCTTT
		5	GGCCCAGTGAGAGCCTCTTCTTCGCCATAGCA
		6	TGTCAACAAGAGCTATATTTGTTTGACCATTA
		7	GATACTGTTTAGAATCGATGGTAAAACTTCAG
		8	GCTGCGGTGCGGCGGGCAACCCTTCACCGCCT

Continued on next page

Table S2: The nucleotide sequence of staple strands in the all-atom models of DNA origami plates

	Number	Sequence
SQ6	1	AATGAATGCCTGGCTCATTTCCCGGTTGATCG
	2	CACTTTGACCGTCTCTAGAGGCGAAAGGAACG
	3	CGCGTGCCTAATACAAGAGTTTTGCCCCAGCA
	4	GGCGAGTTTGGAGAGTGAGCAATCGGCCGGGA
	5	TGTGCAGGTCGAAATGGGATTCAGGAAGATAA
	6	TCAGTTAAATCAAGTAATGTAGCTGATAAATT
	7	TCAAGATATTCACAAAAACATCGCATTATTGG
	8	TGTAGACGACAGCGATTAAGCAAGCTTGATTA
	9	ATTGGCCAGCTGGTTTGATGGGTTGAGTGTTG
	10	TTCCAAAATCCTCATTAATGTAACTCACCATG
	11	CCTGCTGCAAGGTATCGGCCAGGTCACGAATT
	12	TTTGAAAAGCCCACCGTTCTGTAGGTAAAGAT
HC2	1	CGTAATGTTGAGGGCACAATTCCTAATG
	2	AGTGAGCATCCGCTGACGACGGATTGAC
	3	TAGGTGCCAGTGGA
	4	GGTGCCACACATGG
HX2*	1	CGTAATGTTGAGGGCACAATTCCTAATG
	2	AGTGAGCATCCGCTGACGACGGATTGAC
	3	TAGGTGCCAGTGGA
	4	GGTGCCACACATGG
	5[a]	GCGTTGGCCGATTCATTAATG

Continued on next page

Table S2: The nucleotide sequence of staple strands in the all-atom models of DNA origami plates

	Number	Sequence
SQ2 hybrid	1	CGTCAGATGAATTCATTTCAGATTGTATCGCG
	2	TCTGGCCTTCCTAACAGGAAATTACCTGTTAA
	3	GAAAGCCCCAAAGTAGCCAGTTTCAGGTAGCA
	4	AAAGAAGATGATGCGTAGATCTTTTACACAGA
	5	CATAAAAACAGGGAATCTTAAGTTTTGCGGTA
	6	GAAAGATTCATCGCAAAAGACCAACGCTATAA
	7	CGAGAGGCTTTTAGTTGAGACAGAGAGAAACG
	8	AGCGTCTTTCCAAGCCTTTATTTAGGAAATAG

[a] The central helix.

Table S3: The nucleotide sequence of staple strands used in assembly of experimental DNA origami plate systems

Number	Sequence
1	AAATCAAGTTTTTTGGGGGAAAGCCTCATTCACCAGGCGC
2	GGGCGATGGCCCACTAGGGAAGAAATTCATTAGAGTAATC
3	TCCAACGTCAAAGGGCGATGGTGGCATCAGTTGATACATA
4	CAGTTTGGAACAAGAGTCCACTATAAATCAAACGGAACATAGTAAGA
5	GCCCCCGCCGCTACAGGGCGCG
6	GCTTGACGGGTCGAGGACGAGTAG
7	GAAAGGAACGTGAACCATT
8	TCCTGTTTGAAAAACCGCGATTTTAAGAACTG
9	ATCCCTTATTAAAGAACAGGACGT
10	CACCACACGTTAGAATAGGCGCAGGAAACAAA
11	TGGCAAGTCCGATTAAGCGACCTGGCCTGATA
12	GGTTTGCCAACGCGCGCAGAGGGGCAATACTG
13	CCTGAGAGGCGCCAGGTAGCGAGAGAATCCCC
14	CTTTCCTCCCGCCGCGTGTACAGAGTGAATAA
15	ACAGGAGGGTAGCGGTTTCATCAACCCAAATC
16	AATCGGCCCCAGCAGGCTAATGCAGAGATTTA
17	CGTATTGGAGTTGCAGACGAGGCAACATTATT
18	GAGGCCACGCCTGAGTAACCTAAACTACAGAG
19	CAGAATCCTGCTGGTAGTAAAATACATGAGGA
20	TGTCGTGCTTATCCGCGAAGCAAACGAAAGAC
21	CGCTCACTGCCGGAAGAATCAGGTAGCTTCAA
22	CATCACTTCGAGTAAACCAAGCGCACGGTCAA
23	ATCGGCCTTGAGAAGTGTATCATCCTCCATGT

Continued on next page

Table S3: The nucleotide sequence of staple strands used in assembly of experimental DNA origami plate systems

Number	Sequence
24	TGAAATTGCAGCTGCAATAGCGTCGTAATAGT
25	ACATACGAGCCCGCTTTATTCATTGGCTTTTG
26	CCTACATTCATTCTGGAGTTAAAGCAGCTTGA
27	CATTGCAAACCTGAAACCGATATAACAACAAC
28	ATGGTCATATCCTCGCTTTTGCGGTGTAGCTC
29	ATCCCCGGGAACTCGCCCTTTAATAAGTACGG
30	AAAAGGGATTGACGCTAGCAACGGACGAAAGA
31	CCCTTCTGCAGGAAAAGACTTTTTCGTAATGC
32	ACATAACAAGCTGTTTAGGAAGCCGCGGATTG
33	TTTTATCTGTACCGAGTTAATTCGCTTTACCC
34	GAACTGATATTAACACAAAAAAAAAACTTTCA
35	ATTTTTGAGAGCCAGCGAATAATAGAAAGGAA
36	ATAGATGACCATGAAGTTCGCAAATGGGGCGC
37	AAACGATAATCCCCATCGAGTAGACTACTAAT
38	CGGTCAGTAGCCCTAATTCTTAAAGCCGCTTT
39	CACGCTGAATGGCTATCGACAATGTTCGGTCG
40	CAAATATTTTAAACCCTATAATGCATGGCTTA
41	GAAGACAACTTGCCCTTGCAACTATGCTCCTT
42	CAATATCTAATAGATTCGTAACGAACGGAATA
43	CTTGCTGATTGAGGATCCAAAGACGAAAATTC
44	GTATAGATTGCAAGGAAAAGCTAAATACTTTT
45	AGACATCATTAGAGTCAGCAAAATGCAAGGAT
46	TAACAACTGGTCAGTTTGCTAAACGGCTCCAA

Continued on next page

Table S3: The nucleotide sequence of staple strands used in assembly of experimental DNA origami plate systems

Number	Sequence
47	TAATACATACCTCAAATGAGAATAATTTTTTC
48	ACATACATATAGAGTCTTTTCATTTGGTCAAT
49	TCAATGAGCGAAGGTGCATCAATTTTTAGTTT
50	ACGTTATTATTCCTGAACGCAGTAGCCGAACA
51	TTCGACAAAATATAATAAAAGAACAAACGCAA
52	CTGATACCATAACGCTGCCGGAGAGTTCTAGC
53	ATTATCTTCGTCTTCAGTGTAGGTTAGCTATT
54	ATCATCATAATTTTAAAAGACACCTCTAAAGT
55	AATTCATCCTCGTATTAATCAATA
56	TGTAAAAGGTTTAGCTACCCTGTAATCGGTTG
57	TTTCGCGTACTGTTTCATTTCAACTAAGCAAT
58	AATTATTTTTTTACATAATAAGAGATTAACTG
59	ATAATGGACCTGATTGGATAACCCGTAATTGA
60	CAAAGGAGCAGTTAATAAACTAGCGAAAAGCC
61	TGCATATGTCGACATCCAAACAAGGCAAATAT
62	ACAGTACCGCACGTAAAGCAGATATGTTAGCA
63	CGGATTCGAGGGTTAGAACCGAGGTGGCATGA
64	TTCTGCGGAGTGAGATATTCAACCCAGTCAAA
65	AGTAACTAATGTCTGAGGAGAGGGAAAGATTC
66	AGCAAAAGGGAAACAGACGTCAAACGTCTTTC
67	GCAGAGGCGAATAACCCCAATCCAAAATAAAC
68	TGCACTGGAGTATTACCGCCATCAGCTTTCAT
69	CCATCCTGTAAGCGTATTAAATCACAACCCGT

Continued on next page

Table S3: The nucleotide sequence of staple strands used in assembly of experimental DNA origami plate systems

Number	Sequence
70	TTTTTAATAAGATGATACGGGAGACAAGAAAC
71	ATGTGAGTGAATTATTGTCAGAGGACAAGAAT
72	GCAGCGTGTGACCTGGGATAATCAATGTCAAT
73	GATGGGAGGGAAGACTTTGTATAAAGAATCGA
74	GCGATAGCTCCGGCTTCCTTAAATAGCAAATC
75	TTAATTTTTAAATGCTCGAACCTCTTCTAAGA
76	CAGCAAAAGGTAACACTGCATCTGCAGGAAGA
77	ACAGTAGGGATGAACGCACGTTGGCACCGCTT
78	TTTTAACCTTAGATTACTAACGAGAATGAAAA
79	ACTATATGCCCTTAGACAGTTACAAATAAGAA
80	CATGAATTTCAAAACTTGTAGCCAAAAATAAT
81	AACTGCTGGAAACTGCGCGAGTAAGCTCATTT
82	GTTAATTTCGGAATCAGTACCGCATATCCCAT
83	AACGCGAGAGTATCATCTTATCATCCAATCAA
84	GGGATTTGGGGTTGTCTTCGCTATAGGCGATT
85	AAGCGGCAGATCTGGAACTGTTGGCCCAGTCA
86	ATAAACACCATCTTCTCAATAGCACAAGATTA
87	GCCTGTTTAAAACTTTATCCGGTACCGACTTG
88	GTCGTTCAACGCAGACATCGGCCTCCAGTTTG
89	GCCAGGAGGAGCAGGCCTTTCCGGTGTAGATG
90	GAGAATCGATAAGAGAAGAACGCG
91	TAAAGCCAAAGTAATTGACGACAA
92	GATAGATGTGATTCAGGTATTAAC

Continued on next page

Table S3: The nucleotide sequence of staple strands used in assembly of experimental DNA origami plate systems

Number	Sequence
93	CTGCCACTCGCAACACCAAGCTTT
94	AACCACCAGTAAACAGAGAGGTTC
95	CAGAGGCATTTTCGAGCCAGTACCATATTTAAAAATAACTCATCGA
96	TACCGACAAAAGGTAACGCTCAATGTAGAAATCCAAGAA
97	AGATGGCAGACATCATAACGAAGAGTGCTGCATACGCCAG
98	ATAGAAGAATTACAGCATTGTTGAGGGTTTTGAAGGGCG
99	CCTGTTTATCAACAATTGAACAAGAACAACGCAAATAAGA
100	TAAACAACATGTTCAACGAGCACAGTAGGAGAAAAA
101	CAACAGTTCAGGGATTAGGGGGATCGCATTCTTACAACTG
102	ATTATTCGCATTCACTAACGCCTGAGTGTGCAAGTT
103	CCTAATTTGCTAATGCATATAAAG
104	TAATCGGCAATCAGACCTGTCGAA
105	AAGTTGGGCCTCATGCCATCAGAA
106	CGACGTTGGCCAGTGCAGCAATAAAAATG
107	GAACAAGCACCGCGCCGACCTAAAGACTACCT
108	CGGGTATAAGGCTTTTCAAATTTATATA
109	CTGGCGAAACGACAGTCTTTCGCATCCAATTC
110	ATCGGTGCAGCCAGAATGCATGTGCTGG
111	TCGCCATTCAGGGAAACCATCTCAGGCACCAGCAATACATCAA
112	AGGAATCATTAAGCCGTTAAGGCGTTCAACATGT
113	AGATATAGTAAACCAATAATTACTGCTTAATT
114	ACGCGAGGTGTCTTTCATGCGTTATACCAGTA
115	TCGCACTCCGGGCCTCGGACTTGTGGCGATCC

Continued on next page

Table S3: The nucleotide sequence of staple strands used in assembly of experimental DNA origami plate systems

Number	Sequence
116	CTGGTGCCGCTGCGCAACTTATCAGGCTATAT
117	GTTGCTATTACCAACGAGACGCTGAATTACCT
118	CGGGAGGAATTTGCATCCTTGTCAATAT
119	AGGGGACGGGCCTTCCCAATCGTCGTAAACGA
120	GGCGCATAATGTGAGTGTTGATATCTCG
121	TGACCGTAATGCCGTGGGACGAGGATACTGGAAAGCAACGAAG
122	TCCTGAATCTTTTGCACCGTCTGAGATTTAATGGTTTGAAAT
123	CAGAGCCTTTTTGAAGAGGTTGGGATATTTTA
124	AGCCATATCGTTTTAGGATGCAAAAGACAAAG
125	CAACATTACGTAACCGCATCGATTGACGACTG
126	CGGATTCTGGATAGGTGGAAAGAAACTGCGTG
127	TAGCAGCCCGCATTAGGAAACAAAATACAGTA
128	ACGATTTGAACAAACATTTCAACAATAA
129	TCGCGTCTCCCCGGTTAAGGTTACACCAAAGT
130	TTTAACCAGGAAGACCTGTTAACCCGTT
131	AATTCGCATTATAAACGTTAGTTTCTTTCGCTATTACGGGGTT
132	AACAGGGAAGTTTACAGATTCATTTGAGAAGAGTCAATAGTG
133	AACACCCTTTTGTTTATACATAAAAAAACATA
134	GCGCTAATTATTTATCTTGCTTCTGCTATTAA
135	CCAAAAACAATAGGAAGAAGGTGTGCTTGAAA
136	TTAAATTGAATTTTTGTTGCTAAATTGCGCTA
137	AATGAAATGAAAAGTAAACAGAAAGCGGAATT
138	TGAGTTAAGAAGGAAACCTACTGATGGC

Continued on next page

Table S3: The nucleotide sequence of staple strands used in assembly of experimental DNA origami plate systems

Number	Sequence
139[a]	CATATGTAAATATGATCGGATTATTTTGGTTT
140	TGAACGGTAATGCCCGCTGGCTGCTGAA
141	ATTGCCTGAGAATCTACAAGATGCAGGCCAGAGTCTGTAGTGT
142	CCCTTTTTAAAGCAATAGAGATGAATCATCAAGAAAACAAAA
143	AAGTTACCAGCCCAATCGGGAGAAATTACCTG
144	TAATAACGATCAGAGACTTTGAATAAAATCGC
145	TGATAAATTAATCGTACGAACAAGTCAAGCAC
146	TTTGAGAGGTCTGGAGATTACGCAGTTGTTCG
147	AACGTAGAGAAACGCAAAGTTTGAAGGAGCAC
148	TTAAGACTTGTCACAAATCCTCAATAGA
149[b]	TCACCATCACATTATGGAAACTTTATTAGACG
150	AAAAGGGAGCCTTTTTTACATATGAGTA
151	AATGCAATGCCTTAGAACCAAACATCGAAGATTGGGCGTTATC
152	ACATATAAAAAAATACATCAGAAGGATAAAGAAATTGCGTAG
153	AGTTTATTTCCTTATTTTATCAGACATATCAA
154	ATATGGTTGAATACCCCCTGATTGACTTCTGA
155	GCGGGAGATGAGAAAGTGTGAAAAATTCGCAT
156	AAAAATTTTGAGTAATCAGCGATGTGAGTATC
157	TTTGTCGTTGGGATTTGGCAAATCAGGTGAGG
158	TACCAAAATAGCTATAGGCTCTAAAAAAAATA
159	AAAGCCTAAGGTGGTTTATGTGTCTAAT
160	ACAGGCAAGGCCATTAACATGTCTTGTGTGCGAGAAATGACTG
161	ATTTTCTGTACTTTCCAGATATCTTTGTAACATTATCATTTT

Continued on next page

Table S3: The nucleotide sequence of staple strands used in assembly of experimental DNA origami plate systems

Number	Sequence
162	ACAGTTTCATAGTTAGAGAGCCGTTTGCCCGA
163	CAACTAAATACCAGCGTTAGAAGTACAAACAA
164[c]	GAGCTGAACAGAGCATGTTTATAAAAACATTG
165	AGTAGTAGAAAGAATTTGAGCAAAGGTTGAGT
166	AAGGAGCCAGGTGAATAACATCGCCCAGTAAT
167	ACGTTGAGTTGCGCTAGTCTTGATAGAA
168	AACCTGTTTTGCTGAAAATTGGCAATACGATT
169	GACCATTTTAAATACTCTGTAGGATTTA
170	TGATTCCCAATAGTTTCATATCACGAGGTTTTGTTTTATGGAG
171	CTTGCTTTCGTTTAATTGTAAAACAGAACAGTTGAAAGGAAT
172	TACCGATAAAATCTCCCGCCTGCACCCTCAAT
173[d]	CATCGCCCGGAATTGCAGCAAATGAGCATCAC
174	AACATGTTAGATACATGTTTATAAAGATGAAG
175	TGTCTGGATCTGCGAATCTGCAATCTCCATGC
176	TGCGGGATACGAGGGTCAATCGTCAGTAATAA
177	CTGAGGCGACTAAAACGCTCATCAAACT
178	GAGCTTAAAGATTAAGCCTTATTAAACAAGTG
179	TTGATAATCGCGTTCTCGAATCCACACA
180	AGGTCAGGATTAGACCGGAAGTCACAGGTAAAGCCTGGGGTGC
181	CAGCATCGGACGTCACCCTCACACGACATTAAAAATACCGAA
182	GCTTTGAGTTGCAGGGCCAACAGATAATGCGC
183	AGTTTCCAACGCATAAGCGTAAGACAGACAAT
184	TTCAAATAGAGGTCATACTCGCGGCAAAACAT

Continued on next page

Table S3: The nucleotide sequence of staple strands used in assembly of experimental DNA origami plate systems

Number	Sequence
185	AGCGAACCAGAGAGTATACGGCGGTACGGTGG
186	GGCAAAAGCGATTATAAGAGTCTGATAACGTG
187	CACTACGGAGATTTGTTTTTAGAGCTAA
188	CATCAAAATAGACTGGTTAAGGAATAGACATG
189	TGACTATTCATAAATCCAGTCCGGTTTG
190	AGAATGACCATCTTTAAACCACATTAATCTTTTCACCAGTGAG
191	TGACCCCCAGAATACACTCTTTGATTTGAAATGGATTATTTA
192	GTACAACGAAGGCACCAGAAGAACTGGAAATA
193	AATTGTGTTTAAACGGATATCCAGCCGCCAGC
194	CGGAATCGTATAGTCATCACAATTTCGTAATC
195	CTCAAATGAAATCAAACATAAAGTGAGAATGG
196	TCATAAGGATGAACGGCTTAATGCGATTTAGA
197	TACTTAGGCTGACCCACGCTGGTGGCGA
198	AAAATGTTACATTCAACGAGGCGCGAGCGAAA
199	CAAAAGAAGGAATTCAAGCGGTCGGCAAA
200	ACGACGATAAAATCATAACCCCTTCACCCCGAGA
201	AAGAGGACAGGAACCGAAGAGCACGTTCCATCACGCAAATTA
202	ATAGGCTGCCGGAACGCAGAGCGGTAATCAGT
203	TTGACAAGCGAAATCCAGGGATTTCGGTACGC
204	ACGCCAAAAGTTTTGCGGGAGAGGGGGAAACC
205	GCAACACTAACCAAAAGTGGTTTTTTGCGTTG
206	GGCTTGCCACACCAGATGCCGTAAAGCACT
207	AACGTAATGGTTTAATCACCC

Continued on next page

Table S3: The nucleotide sequence of staple strands used in assembly of experimental DNA origami plate systems

Number	Sequence
208	GGAATACCTACCTTATGTCTATCA
209	ACAGGTATACCAGTCGTGGAC
210	TAAATTGGGCTTGAGACAAAGCTGCGGCGAACCGCGTAAC
211	TCAACTTTAATCATTGTGAATAACCGGATAGCGAAAGTAGGGCGC
212	GCTCATTAGAAAGATTTTCCGAAATCCACGCT
213	TGGGAAGAAAAATCTAACGAACTAAAGAATAGCGCCTGGC
214	AAAAGGGCGACATTCAACCGATTGAGGGAGGG
215	AAGGTAAATATTGACGGAAATTATTCATTAAA
216	GGTGAATTATCACCGTCACCGACTTGAGCCAT
217	TTGGGAATTAGAGCCAGCAAAATCACCAGTAG
218	CACCATTACCATTAGCAAGGCCGGAAACGTCA
219	CCAATGAAACCATCGATAGCAGCACCGTAATC
220	AGTAGCGACAGAATCAAGTTTGCCTTTAGCGT
221	CAGACTGTAGCGCGTTTTCATCGGCATTTTCG
222	GTCATAGCCCCCTTATTAGCGTTTGCCATCTT
223	TTCATAATCAAAATCACCGGAACCAGAGCCAC
224	CACCGGAACCGCCTCCCTCAGAGCCGCCACCC
225	TCAGAACCGCCACCCTCAGAGCCACCACCCTC
226	AGAGCCGCCACCAGAACCACCACCAGAGCCGC
227	CGCCAGCATTGACAGGAGGTTGAGGCAGGTCA
228	GACGATTGGCCTTGATATTCACAAACAAATAA
229	ATCCTCATTAAAGCCAGAATGGAAAGCGCAGT
230	CTCTGAATTTACCGTTCCAGTAAGCGTCATAC

Continued on next page

Table S3: The nucleotide sequence of staple strands used in assembly of experimental DNA origami plate systems

Number	Sequence
231	ATGGCTTTTGATGATACAGGAGTGTACTGGTA
232	ATAAGTTTTAACGGGGTCAGTGCCTTGAGTAA
233	CAGTGCCCGTATAAACAGTTAATGCCCCCTGC
234	CTATTTCGGAACCTATTATTCTGAAACATGAA
235	AGTATTAAGAGGCTGAGACTCCTCAAGAGAAG
236	GATTAGGATTAGCGGGGTTTTGCTCAGTACCA
237	GGCGGATAAGTGCCGTCGAGAGGGTTGATATA
238	AGTATAGCCCGGAATAGGTGTATCACCGTACT
239	CAGGAGGTTTAGTACCGCCACCCTCAGAACCG
240	CCACCCTCAGAACCGCCACCCTCAGAGCCACC
241	ACCCTCATTTTCAGGGATAGCAAGCCCAATAG
242	GAACCCATGTACCGTAACACTGAGTTTCGTCA
243	CCAGTACAAACTACAACGCCTGTAGCATTCC

[a] Cy5-labeled staple (‘perpendicular’)

[b] Cy3-labeled staple

[c] Cy5-labeled staple (‘parallel’)

[d] Cy5-labeled staple (‘diagonal’)

Table S4: The nucleotide sequence of staple strands used in assembly of the Cuboid X in experiments (the leash is shown in green)

Number	Sequence
1	GGGCGATGAAGCACTAACCAGTCATGGATTATGCCAGCTT
2	ACGTGGACTCCAACGTTGTTGTTCGATTAAGTTTGTAAAAGACAGTAT
3	GTGCCGTAGCCCACTAGAAAGCGTAAGAATACGTCTTTAA
4	GGAGCCCCCAAAGGGCCGCTATTACGCCAGCTTCGGTGCG
5	CCGGCGAACAGCAGGCATTACCGCCTTGCTGGCAAATATC
6	GGGTTGAGCGAAATCGCTGCAGGTAATTCGTAGTTGGTGT
7	GCGCTGGCCGTGGCGAGTCTGAAACACGACCAGAACCACC
8	GGTGGTTCCGATTTAGTCACGACGTGGGTAACAACCAGGC
9	GTTTGCCCGCTACAGGAACCGTTGAAGAGTCTTCATCAAC
10	CCTGAGAGTTCACCAGGAAATTGTCGGAAGCATAATTCGC
11	AATGCGCCAAGTGTAGCTATCGGCCAGCCATTGCAACAGT
12	CTTTGACGAGTTGCAGCGAGCTCGCGACTCTATGAAAAAT
13	TTAGAATCAAACCTGTCTCACTGCCCGCTTTCTTGTAAAC
14	TTTTTCTTGCCAACGCTGAGTGAGCTAACTCATTAAATTT
15	TAGACAGGCAGTCGGGAGAGCGGGCCGAGTAATAGCAATAGGAATTGA
16	ATGAATCGAGCACGTAATACGAGCTATCCGCTCGTCGGAT
17	AACGGTACTGAGGCCAAGCTAAACCCGCGCTT
18	CACACAACTAACGTGCTATGGTTG
19	CTTCTTTGAACTCAAACGGTCACGGCGCTAGG
20	CGCAAATTGCGCGTACTTTCCTCG
21	TCCTGTGTTGAGACGGCAGGGTGG
22	CCGGGTACCAAGCGGTTGTTTGAT
23	GCAACAGGGCTCAATCGAAAGGAAGGGTCGAG

Continued on next page

Table S4: The nucleotide sequence of staple strands used in assembly of the Cuboid X in experiments (the leash is shown in green)

Number	Sequence
24	AGAACAATGAAAATCCCCACGCTG
25	TTGCATGCGCAAAATCCGCCTGGC
26	TTTCCCAGAGCTTGACCCCTAAAG
27	GTAATAAATCTGACCTCGTGAACC
28	GCAGATTCAATCGGAAGGGGAAAG
29	TGCAAGGCCAGTTTGGCCGAGATA
30	GACAATATGAAAAACCGTCTATCA
31	CCTAAAACAGAACCCTAGGGACAT
32	TGCGCGAACAGTAACAGTACCTTTATTGCTTT
33	GGCCTCTTTAGAACCCTCATATATCAAGGATA
34	ATTAAAAAGAGGTGAGATTTTGACAAAAACGC
35	TCCGGCACTTTGCACGTTAGAACCAAGCCTCA
36	AAAGCGCCTAGGTAAACAAATCACGCAAGGCA
37	AGCAGAAGTGGAAGGGTAAAACAGTTACCTGA
38	CGGCCTCAGAGACAGTGATTCAAACCAAAAAC
39	AGTATTAATCTGGTCAAGTAGAAGATTAGTAA
40	GCCACGCTTGATTATCGGAGCGGAGTGAATAA
41	AGATGGGCGCTGATAAGATCTACAATAGGAAC
42	AAACCCTCCACCAGAAAGATGATGCATTTAAC
43	CTAAAGCATTTTGAGAATTAATGCAATGGAAA
44	AAATCAACTATCTTTAATAATCAGGCCAGAAT
45	ATTAAATGTTTGCCCGAATTCGACGTTTAGTA
46	TCTCCGTGTCTGGAGCACTAGCATGCCCGGAA

Continued on next page

Table S4: The nucleotide sequence of staple strands used in assembly of the Cuboid X in experiments (the leash is shown in green)

Number	Sequence
47	GGAAGGTTTTACAAACAACGTTATCCTTGAAA
48	GTCTGGCCATCGTAAAAAACAAGATCAGAACC
49	AATTCGCACATTAATTGCGTTGCGCGTGCCAGCTGCATTA
50	GTTAATATTAAGCAAATATTTAAAATTTATCA
51	TTGTTAAAATCAGAAAAGCCCCAAGTTTTGCT
52	TAGAGCCGATTAGACTATCTAAAAAGTTGAAA
53	GAACGGTATTCCTGTATAACAACCCACAATTC
54	TTAAATCCTGAGCGAGGCCAGCTTGTCCATCA
55	CCTGAGAGGGAACAAAATCAAAAATAAAGTGT
56	TAATTTTAAAAGAAACAATCAATACACCGCCT
57	GTAGCTATTCACCTTGGCAGCAAAGAGGATCC
58	CATATTCCGAGAGCCACTGAACCTTAATATCC
59	CCGTTCTAGCATCGTATAGGTCACATCATGGT
60	GCAATTCACTGAATAAATAAAACATACCGAAC
61	AAAGGCCGGGAAGATCGTGCCGGAGCCAGGGT
62	CAAAATTACGCTTCTGGCACTCCATTACATTG
63	GTAATGTGATTCGCCAGGGACGACCGACGGCC
64	AAATAAAGTGAATATACTGATAGC
65	GAGAAACATTTTGAATGGCTATTAGTGGCACA
66	AATCGCGCACGTCAGAAAATTGCG
67	GAATACCAAGAGCCGCCGCCAGCACACCAGAA
68	AAAATTTTGCAGGTCAGACGATTGGCCACCCT
69	GAATTATTAAACAAACTTATACTTTCAATATA

Continued on next page

Table S4: The nucleotide sequence of staple strands used in assembly of the Cuboid X in experiments (the leash is shown in green)

Number	Sequence
70	GAGCATAACGCCAACAATTGAGAAAATAATAT
71	ATTATGACCCTCATTAACCGTTCCGGAACCAG
72	GCAAAAGAAGGGCTTATGTAATTTCAACATGT
73	AAGAATTACTGAATTTAAGCCAGATTATCAAC
74	AAAACAAACGTCGCTATGCGGAACAAAGTTTG
75	AATTTCATAAGCCTGTCACCGGAAGCGTCAGA
76	CCATGTACGATACAGGTGCCTTGAAATCAGTA
77	CCTTGCTTAGAATAAATTAGTATCTCTTTCCT
78	CAGTACATGGGGTCAGAGTGTACTTTCGGTCA
79	AATTTTCCGATTAAGATTAGAAGTTCAATAGA
80	CCGCCACCTCATCTTCTTTTCAAAGATATAGA
81	GCCACCCTTGCCCCCTAAAGTATTTACCATTA
82	ACATAGCGAGAAAACTTGACCTAAAACAAGCA
83	TAGGTGTAGAAACATGGCCTATTTAATCATTA
84	AGACTACCAAACAGGAAGATTGTATTTGTTAA
85	AAATCATATAGGTTGGGTTATATAGAAATTAT
86	CAGTACCAGATTAGGATTAGCGGGCACCGACT
87	ACTATATGAGAACGCGATAGCTTACTTAGAAT
88	ATTATTCTTCACCGTACGCCACCCGAATCGAT
89	AGTTAATTCTCAGAACCTCAGGAGAACTCGTA
90	ACAGTTAACAGAGCCATAAGTATAGTCAATCA
91	ATTTAATGGTTAAATACTGTAAATATTAATTA
92	GTTTTAACAAATCAATCCTTTTTTCGGAGAGG

Continued on next page

Table S4: The nucleotide sequence of staple strands used in assembly of the Cuboid X in experiments (the leash is shown in green)

Number	Sequence
93	ACTAGAAATTGAATTAATATGTGAATTATCAT
94	CTTTTGATCGTAACACCAAGCCCAAAGGCTAT
95	ATATGCGTTCAACAGTAGATGATGCATTTCAA
96	CGCAGTCTGCAAAATTCGGTTGTAAGGGTGAG
97	TTTAACAAAGCTAAATAAGCAATATACCATAT
98	AAATAAATCCTGTAATTCATACAGCATCAATA
99	AGGCAGAGGTACCGACAGTTACAA
100	AGGTTGAGATAACGGATTCGCCTGTACATCGG
101	AAGTAATTAATATAAAGCATTTTC
102	CCACCACCAATAATAAGAGCAAGA
103	CAGAGCCATAGCTATCTTACCGAA
104	TCAGCTAACAAAGTCAGGAGAATT
105	AGCCACCAAGCCGAACTAATAACG
106	CCCATCCTATTAGACGGAGGGTAA
107	AATAGATAAAACGCAAAAAGTTAC
108	CTGTAGCGGTTTAACGAATCCAAA
109	TAGCCCCCAAGACTCCTACATACA
110	TATCATTCTTTATCCCTCAAAAAT
111	GCGACAGAGTAGAAAATTATTACG
112	AGCCGTTTACCAACGCAGCTACAA
113	GCAAGGCCGCAAAGACTAGAAAAT
114	AGGCTTATTTGCACCCTAACGAGC
115	CCGCGCCCACAATCAAACCACGGA

Continued on next page

Table S4: The nucleotide sequence of staple strands used in assembly of the Cuboid X in experiments (the leash is shown in green)

Number	Sequence
116	ATCACCGTTTTTTAACCTCCGGCTGGTCTGAG
117	TCATTAAAAAGGTAAATATTGACG
118	TGAGCCATAAAAGGGCGACATTCA
119	ACCGATTGATTTTGTCAATAGCAAATCGTAGGCGGAACCT
120	CCGACTTGTTGCTATTCCGGTATTTCATCGAG
121	AAGATTAGCGGGAGGTCGTTTTAGCGAACCTC
122	TTTTATCCAGGGAGGGGGTGAATT
123	TCATATGGCCAAAGACTTGGGAAT
124	ATAAGTTTTAGCAAACATCAAGTTTCGGCATTGGTAATAA
125	GTCTTTCCCCATATTACAAGAACGATCGGCTG
126	ATAAACAGAGAGCCTATACCGCACCTAAGAACCAAGACAATAAATGCT
127	TAAGAAACTGAATCTTTTATTTTCGCAAATCATATATTTT
128	TAAAGGTGAAAGAAACGGAAACGTAGCACCATAAGAGGCT
129	CAGTATGTAACCGAGGAGTCCTGAGCGCCTGTATGGAAAG
130	GAAAATAGGGAAGCGCAATTTACGACAATAAA
131	AAAAACAGCAGCCTTTAATCAATAGGTATTAAAATAAGGCGTTTGAAA
132	AACTGAACGATTTTTTCGTTTTCATGCCTTTATCATAATT
133	GAATACCCGCATGATTTTATTAGCAGCACCGTGTAACAGT
134	CAGAAGGAAATAGCAACCACCCTCAGAGCCGCTTGACAGG
135	TTGAGCGCTTAAGCCCAAAAGGTA
136	GAATTGAGTAATATCAAGACGACGAGCATGTAGCCAACGCTATACAAA
137	AACAATGAACCCTGAATGCAGAACACAAGAAATCGCCATA
138	GCCCTTTTAAGCAGATCCGGAACCAAATCACCAGTAAGCG

Continued on next page

Table S4: The nucleotide sequence of staple strands used in assembly of the Cuboid X in experiments (the leash is shown in green)

Number	Sequence
139	CGTCACCAGTACAAACTACAACGCCTGTAGCATTCCACAG
140	ACAGCCCTCATAGTTAGCGTAACGATCTAAAGTTTTGTCG
141	TCTTTCCAGACGTTAGTAAATGAATTTTCTGTATGGGATT
142	TTGCTAAACAACTTTCAACAGTTTCAGCGGAGTGAGAATA
143	GAAAGGAACAACTAAAGGAATTGCGAATAATAATTTTTTC
144	ACGTTGAAAATCTCCAAAAAAAAGGCTCCAAAAGGAGCCT
145	TTAATTGTATCGGTTTATCAGCTTGCTTTCGAGGTGAATT
146	TCTTAAACAGCTTGATACCGATAGTTGCGCCGACAATGAC
147	AACAACCATCGCCCACGCATAACCGATATATTCGGTCGCT
148	GAGGCTTGCAGGGAGTTAAAGGCCGCTTTTGCGGGATCGT
149	CACCCTCAGCAGCGAAAGACAGCATCGGAACGAGGGTAGC
150	AACGGCTACAGAGGCTTTGAGGACTAAAGACTTTTTCATG
151	AGGAAGTTTCCATTAAACGGGTAAAATACGTAATGCCACT
152	ACGAAGGCACCAACCTAAAACGAAAGAGGCAAAAGAATAC
153	ACTAAAACACTCATCTTTGACCCCCAGCGATTATACCAAG
154	CGCGAAACAAAGTACAACGGAGATTTGTATCATCGCCTGA
155	TAAATTGTGTCGAAATCCGCGACCTGCTCCATGTTACTTA
156	GCCGGAACGAGGCGCAGACGGTCAATCATAAGGGAACCGA
157	ACTGACCAACTTTGAAAGAGGACAGATGAACGGTGTACAG
158	ACCAGGCGCATAGGCTGGCTGACCTTCATCAAGAGTAATC
159	TTGACAAGAACCGGATATTCATTACCCAAATCAACGTAAC
160	AAAGCTGCTCATTCAGTGAATAAGGCTTGCCCTGACGAGA
161	AACACCAGAACGAGTAGTAAATTGGGCTTGAGATGGTTTA

Continued on next page

Table S4: The nucleotide sequence of staple strands used in assembly of the Cuboid X in experiments (the leash is shown in green)

Number	Sequence
162	ATTTCAACTTTAATCATTGTGAATTACCTTATGCGATTTT
163	AGAACTGGCTCATTATACCAGTCAGGACGTTGGGAAGAA
164	AAATCTACGTTAATAAAACGAACTAACGGAACAACATTAT
165	TACAGGTAGAAAGATTCATCAGTTGAGATTTAGGAATACC
166	ACATTCAACTAATGCAGATACATAACGCCAAAAGGAATTA
167	CGAGGCATAGTAAGAGCAACACTATCATAACCCTCGTTTA
168	CCAGACGACGATAAAAACCAAAATAGCGAGAGGCTTTTGC
169	AAAAGAAGTTTTGCCAGAGGGGGTAATAGTAAAATGTTTA
170	GACTGGATAGCGTCCAATACTGCGGAATCGTCATAAATAT
171	TCATTGAATCCCCCTCAAATGCTTTAAACAGTTCAGAAAA
172	CGAGAATGACCATAAATCAAAAATCAGGTCTTTACCCTGA
173	CTATTATAGTCAGAAGCAAAGCGGATTGCATCAAAAAGAT
174	TAAGAGGAAGCCCGAAAGACTTCAAATATCGCGTTTTAAT
175	TCGAGCTTCAAAGCGAACCAGACCGGAAGCAAACTCCAAC
176	AGGTCAGGATTAGAGAGTACCTTTAATTGCTCCTTTTGAT
177	AAGAGGTCATTTTTGCGGATGGCTTAGAGCTTAATTGCTG
178	AATATAATGCTGTAGCTCAACATGTTTTAAATATGCAACT
179	AAAGTACGGTGTCTGGAAGTTTCATTCCATATAACAGTTG
180	ATTCCCAATTCTGCGAACGAGTAGATTTAGTTTGACCATT
181	AGATACATTTCGCAAATGGTCAATAACCTGTTTA
182	GCTATATTTTCATTTGGGGCGCGAGCTGAAAAG
183	GTGGCATCAATTCTACTAATAGTAGTAGCATTA

Table S5: The nucleotide sequence of staple strands used in assembly of the Cuboid Y in experiments (the leash is shown in green)

Number	Sequence
1	GGGCGATGAAGCACTAACCAGTCATGGATTATGCCAGCTT
2	ACGTGGACTCCAACGTTGTTGTTCGATTAAGTTTGTAAAAGACAGTAT
3	GTGCCGTAGCCCACTAGAAAGCGTAAGAATACGTCTTTAA
4	GGAGCCCCCAAAGGGCCGCTATTACGCCAGCTTCGGTGCG
5	CCGGCGAACAGCAGGCATTACCGCCTTGCTGGCAAATATC
6	GGGTTGAGCGAAATCGCTGCAGGTAATTCGTAGTTGGTGT
7	GCGCTGGCCGTGGCGAGTCTGAAACACGACCAGAACCACC
8	GGTGGTTCCGATTTAGTCACGACGTGGGTAACAACCAGGC
9	GTTTGCCCGCTACAGGAACCGTTGAAGAGTCTTCATCAAC
10	CCTGAGAGTTCACCAGGAAATTGTCGGAAGCATAATTCGC
11	AATGCGCCAAGTGTAGCTATCGGCCAGCCATTGCAACAGT
12	CTTTGACGAGTTGCAGCGAGCTCGCGACTCTATGAAAAAT
13	TTAGAATCAAACCTGTCTCACTGCCCGCTTTCTTGTAAAC
14	TTTTTCTTGCCAACGCTGAGTGAGCTAACTCATTAAATTT
15	TAGACAGGCAGTCGGGAGAGCGGGCCGAGTAATAGCAATAGGAATTGA
16	ATGAATCGAGCACGTAATACGAGCTATCCGCTCGTCGGAT
17	AACGGTACTGAGGCCAAGCTAAACCCGCGCTT
18	CACACAACTAACGTGCTATGGTTG
19	CTTCTTTGAACTCAAACGGTCACGGCGCTAGG
20	CGCAAATTGCGCGTACTTTCCTCG
21	TCCTGTGTTGAGACGGCAGGGTGG
22	CCGGGTACCAAGCGGTTGTTTGAT
23	GCAACAGGGCTCAATCGAAAGGAAGGGTCGAG

Continued on next page

Table S5: The nucleotide sequence of staple strands used in assembly of the Cuboid Y in experiments (the leash is shown in green)

Number	Sequence
24	AGAACAATGAAAATCCCCACGCTG
25	TTGCATGCGCAAAATCCGCCTGGC
26	TTTCCCAGAGCTTGACCCCTAAAG
27	GTAATAAATCTGACCTCGTGAACC
28	GCAGATTCAATCGGAAGGGGAAAG
29	TGCAAGGCCAGTTTGGCCGAGATA
30	GACAATATGAAAAACCGTCTATCA
31	CCTAAAACAGAACCCTAGGGACAT
32	TGCGCGAACAGTAACAGTACCTTTATTGCTTT
33	GGCCTCTTTAGAACCCTCATATATCAAGGATA
34	ATTAAAAAGAGGTGAGATTTTGACAAAAACGC
35	TCCGGCACTTTGCACGTTAGAACCAAGCCTCA
36	AAAGCGCCTAGGTAAACAAATCACGCAAGGCA
37	AGCAGAAGTGGAAGGGTAAAACAGTTACCTGA
38	CGGCCTCAGAGACAGTGATTCAAACCAAAAAC
39	AGTATTAATCTGGTCAAGTAGAAGATTAGTAA
40	GCCACGCTTGATTATCGGAGCGGAGTGAATAA
41	AGATGGGCGCTGATAAGATCTACAGGTGGCAT
42	AAACCCTCCACCAGAAAGATGATGCATTTAAC
43	CTAAAGCATTTTGAGAATTAATGCAATGGAAA
44	AAATCAACTATCTTTAATAATCAGGCCAGAAT
45	ATTAAATGTTTGCCCGAATTCGACGTAGATTT
46	TCTCCGTGTCTGGAGCACTAGCATATATAACA

Continued on next page

Table S5: The nucleotide sequence of staple strands used in assembly of the Cuboid Y in experiments (the leash is shown in green)

Number	Sequence
47	GGAAGGTTTTACAAACAACGTTATCCTTGAAA
48	GTCTGGCCATCGTAAAAAACAAGACAAATGGT
49	AATTCGCACATTAATTGCGTTGCGCGTGCCAGCTGCATTA
50	GTTAATATTAAGCAAATATTTAAAATTTATCA
51	TTGTTAAAATCAGAAAAGCCCCAAGCTCAACA
52	TAGAGCCGATTAGACTATCTAAAAAGTTGAAA
53	GAACGGTATTCCTGTATAACAACCCACAATTC
54	TTAAATCCTGAGCGAGGCCAGCTTGTCCATCA
55	CCTGAGAGGGAACAAAATCAAAAATAAAGTGT
56	TAATTTTAAAAGAAACAATCAATACACCGCCT
57	GTAGCTATTCACCTTGGCAGCAAAGAGGATCC
58	CATATTCCGAGAGCCACTGAACCTTAATATCC
59	CCGTTCTAGCATCGTATAGGTCACATCATGGT
60	GCAATTCACTGAATAAATAAAACATACCGAAC
61	AAAGGCCGGGAAGATCGTGCCGGAGCCAGGGT
62	CAAAATTACGCTTCTGGCACTCCATTACATTG
63	GTAATGTGATTCGCCAGGGACGACCGACGGCC
64	AAATAAAGTGAATATACTGATAGC
65	GAGAAACATTTTGAATGGCTATTAGTGGCACA
66	AATCGCGCACGTCAGAAAATTGCG
67	GAATACCACGGAATCGTCATAAATATAGCGTC
68	AAAATTTTTCAAATGCTTTAAACACAGAGGGG
69	GAATTATTAAACAAACTTATACTTTCAATATA

Continued on next page

Table S5: The nucleotide sequence of staple strands used in assembly of the Cuboid Y in experiments (the leash is shown in green)

Number	Sequence
70	GAGCATAAGAGAGGGTAGTACCAGGTTTCGTC
71	ATTATGACTCAAAAATCAAAGCGGCCAGACGA
72	GCAAAAGATTTTGCTCTGATATAAAGAGCCAC
73	AAGAATTAGTCAGAAGCAGGTCTTGCCCAATA
74	AAAACAAACGTCGCTATGCGGAACAAAGTTTG
75	AATTTCATATTCTGAACCCCTGCCAATACCAC
76	CAATTCTACCCGAAAGAAGCGAACCAGGTAGA
77	CCTTGCTTGTTAATGCACATGAAATAGTTAGC
78	CAGTACATGAGCTTCAACTTCAAAGCCAAAAG
79	AATTTTCCGATTAAGATTAGAAGTTCAATAGA
80	AGTTTGACAGGAGTGTGTCATACACAACTAAA
81	CAATAACCCAGGATTAGGTCATTTCGTTGGGA
82	ACATAGCGCAGTAAGCACTGGTAATTTTCTGT
83	GTTGATTCTGATAAGAGAGAGTACAACAGTTT
84	CAGGTCAGAAACAGGAAGATTGTATTTGTTAA
85	AAATCATATTCACAAACAAATAAATGGGCTTG
86	TGTTTTAATGAATATAATGCTGTACATTGTGA
87	TCCTCATTTACCGTTCATAGCTTACTTAGAAT
88	GCTCCTTTCCAATTCTACATTTCGGAATCGAT
89	GATGATACCATTAGATGCGAACGAAACTCGTA
90	CAACAGGTTGTTTAGCTTCATTCCGTCAATCA
91	TAAGTTTTTATAAACACTGTAAATATTAATTA
92	TTTAATTCAAATCAATCCTTTTTTCGGAGAGG

Continued on next page

Table S5: The nucleotide sequence of staple strands used in assembly of the Cuboid Y in experiments (the leash is shown in green)

Number	Sequence
93	AACCTATTTTGAATTAATATGTGAATTATCAT
94	AGAGGAAGCTAATAGTGCTGAAAAAAGGCTAT
95	GTATTAAGTAGCGGGGAGATGATGCATTTCAA
96	CTATTATAGCAAAATTCGGTTGTAAGGGTGAG
97	GTGCCGTCAGCTAAATAAGCAATATACCATAT
98	ACCATAAACCTGTAATTCATACAGCATCAATA
99	GTATAGCCTAGTACCGAGTTACAA
100	AATCCCCCATAACGGATTCGCCTGTACATCGG
101	AGAACCGCAGGAGGTTCGGAATAG
102	CAATACTGACACTAAAACACTCAT
103	GTAATAGTTTATACCAAGCGCGAA
104	CACCCTCAAAACGGGTCTTTTTCA
105	CGATAAAATCGCCTGAGTTACTTA
106	ACCAGTACACTAAAGAAAAATACG
107	GGAACCCATGCTCCATTAAATTGT
108	ATTCAACTGTCACCCTGTTAAAGG
109	GAATTACGCATAAGGGTGAACGGT
110	GTAACGATTGCAGGGACAGCAGCG
111	AAGATTCAAGGACAGAAACCGAAC
112	ATGGGATTAGTTGCGCTTTCTTAA
113	AGAAAAATGACCTTCAATTACCCA
114	GGAATTGCGAGGTGAACGACAATG
115	CAGCGGAGGGATATTCTCAAGAGT

Continued on next page

Table S5: The nucleotide sequence of staple strands used in assembly of the Cuboid Y in experiments (the leash is shown in green)

Number	Sequence
116	ACTTTAATACGATTGGCCTTGATA
117	AGATGGTTAGAACGAGTAGTAAAT
118	ATTACCTTAGTGAATAAGGCTTGC
119	CCTGACGACAAGAACCTGAGAATACAACTTTCCTTTAATT
120	AGGCTCCATTGCTTTCGAATAATATAAATGAA
121	TTATCAGCAAAGGAGCAAAATCTCCAAAAAAA
122	ACAGCTTGGAAACACCTAATTTCA
123	AATCAACGGCTCATTCATGCGATT
124	AATCTTGATTTGAAAGTCAGTTGATACATAACTATCGCGT
125	ACAACAACCTGAGGCTCTAAAGTTAGCCCTCA
126	TTCGGTCGCATCGCCCGACGTTAGATTTTTTCTCTGAATTAAAGCCAG
127	CCGCTTTTATACCGATTTGCTAAAGAAAGGAATGGCTTTT
128	GTACAGACGGCTGGCTCTACGTTAAGTCAGGATTGCGGAT
129	TGACCAACCCGCGACCTGTACCGTGATAGCAATACCCTGA
130	AAAGACAGCTTTGAGGAAACTACACCACCCTC
131	TACAGAGGCATCGGAACCACAGACTTGTCGTCAGTGCCCGAACGGGGT
132	TGAGGAAGGCGGGATCAATGCAGAGATTTAGGTATTTCGG
133	GCCGGAACCGGTCAATAGGCATAGCATTATTACAGACCGG
134	GTCGAAATCCCAGCGAAAAATGTTTAGACTGGATTCATTG
135	TAATGCCAAAAAGAATCCACCCTC
136	AAAGAGGCCTACGAAGCAGAACCGACGCCTGTATTAGGATAGGCTGAG
137	CTTTGACCTTTCCATTTTTTCAGGAACACTGAGCGGATAA
138	ACAAAGTATTGTATCAACCAAAATCTCGTTTAATTGCATC

Continued on next page

Table S5: The nucleotide sequence of staple strands used in assembly of the Cuboid Y in experiments (the leash is shown in green)

Number	Sequence
139	GTCTGAGAGACTACCTTTTTAACCTCCGGCTTAGGTTGGG
140	TTATATAACTATATGTAAATGCTGATGCAAATCCAATCGC
141	AAGACAAAGAACGCGAGAAAACTTTTTCAAATATATTTTA
142	GTTAATTTCATCTTCTGACCTAAATTTAATGGTTTGAAAT
143	ACCGACCGTGTGATAAATAAGGCGTTAAATAAGAATAAAC
144	ACCGGAATCATAATTACTAGAAAAAGCCTGTTTAGTATCA
145	TATGCGTTATACAAATTCTTACCAGTATAAAGCCAACGCT
146	CAACAGTAGGGCTTAATTGAGAATCGCCATATTTAACAAC
147	GCCAACATGTAATTTAGGCAGAGGCATTTTCGAGCCAGTA
148	ATAAGAGAATATAAAGTACCGACAAAAGGTAAAGTAATTC
149	TGTCCAGACGACGACAATAAACAACATGTTCAGCTAATGC
150	AGAACGCGCCTGTTTATCAACAATAGATAAGTCCTGAACA
151	AGAAAAATAATATCCCATCCTAATTTACGAGCATGTAGAA
152	ACCAATCAATAATCGGCTGTCTTTCCTTATCATTCCAAGA
153	ACGGGTATTAAACCAAGTACCGCACTCATCGAGAACAAGC
154	AAGCCGTTTTTATTTTCATCGTAGGAATCATTACCGCGCC
155	CAATAGCAAGCAAATCAGATATAGAAGGCTTATCCGGTAT
156	TCTAAGAACGCGAGGCGTTTTAGCGAACCTCCCGACTTGC
157	GGGAGGTTTTGAAGCCTTAAATCAAGATTAGTTGCTATTT
158	TGCACCCAGCTACAATTTTATCCTGAATCTTACCAACGCT
159	AACGAGCGTCTTTCCAGAGCCTAATTTGCCAGTTACAAAA
160	TAAACAGCCATATTATTTATCCCAATCCAAATAAGAAACG
161	ATTTTTTGTTTAACGTCAAAAATGAAAATAGCAGCCTTTA

Continued on next page

Table S5: The nucleotide sequence of staple strands used in assembly of the Cuboid Y in experiments (the leash is shown in green)

Number	Sequence
162	CAGAGAGAATAACATAAAAACAGGGAAGCGCATTAGACGG
163	GAGAATTAACTGAACACCCTGAACAAAGTCAGAGGGTAAT
164	TGAGCGCTAATATCAGAGAGATAACCCACAAGAATTGAGT
165	TAAGCCCAATAATAAGAGCAAGAAACAATGAAATAGCAAT
166	AGCTATCTTACCGAAGCCCTTTTTAAGAAAAGTAAGCAGA
167	TAGCCGAACAAAGTTACCAGAAGGAAACCGAGGAAACGCA
168	ATAATAACGGAATACCCAAAAGAACTGGCATGATTAAGAC
169	TCCTTATTACGCAGTATGTTAGCAAACGTAGAAAATACAT
170	ACATAAAGGTGGCAACATATAAAAGAAACGCAAAGACACC
171	ACGGAATAAGTTTATTTTGTCACAATCAATAGAAAATTCA
172	TATGGTTTACCAGCGCCAAAGACAAAAGGGCGACATTCAA
173	CCGATTGAGGGAGGGAAGGTAAATATTGACGGAAATTATT
174	CATTAAAGGTGAATTATCACCGTCACCGACTTGAGCCATT
175	TGGGAATTAGAGCCAGCAAAATCACCAGTAGCACCATTAC
176	CATTAGCAAGGCCGGAAACGTCACCAATGAAACCATCGAT
177	AGCAGCACCGTAATCAGTAGCGACAGAATCAAGTTTGCCT
178	TTAGCGTCAGACTGTAGCGCGTTTTCATCGGCATTTTCGG
179	TCATAGCCCCCTTATTAGCGTTTGCCATCTTTTCATAATC
180	AAAATCACCGGAACCAGAGCCACCACCGGAACCGCCTCCC
181	TCAGAGCCGCCACCCTCAGAACCGCCACCCTCAG
182	AGCCACCACCCTCAGAGCCGCCACCAGAACCACC
183	ACCAGAGCCGCCGCCAGCATTGACAGGAGGTTGA

Table S6: Conversion of experimental buffer concentrations

0.5×TBE	44.5 mM	Tris-Borate
	1 mM	EDTA
1×TE	10 mM	Tris HCl
	1 mM	EDTA

References

1. Aksimentiev, A.; Heng, J. B.; Timp, G.; Schulten, K. Microscopic Kinetics of DNA Translocation through Synthetic Nanopores. *Biophys. J.* **2004**, *87*, 2086–2097.

2. Hunter, J. D. Matplotlib: A 2D Graphics Environment. *Comput. Sci. Eng.* **2007**, *9*, 90–95.

3. Yoo, J.; Aksimentiev, A. Competitive Binding of Cations to Duplex DNA Revealed through Molecular Dynamics Simulations. *J. Phys. Chem. B* **2012**, *116*, 12946–12954.